Supporting Information

Mechanism of Photoinduced Metal-Free Atom Transfer Radical Polymerization: Experimental and Computational Studies

Xiangcheng Pan[1], Cheng Fang[2], Marco Fantin[1,3], Nikhil Malhotra[1], Woong Young So[1], Linda A. Peteanu[1], Abdirisak A. Isse[3], Armando Gennaro[3,*], Peng Liu[2,*], and Krzysztof Matyjaszewski[1,*]

[1]Department of Chemistry, Carnegie Mellon University, Pittsburgh, Pennsylvania, 15213, United States

[2]Department of Chemistry, University of Pittsburgh, Pittsburgh, Pennsylvania, 15260, United States

[3]Department of Chemical Sciences, University of Padova, via Marzolo 1, 35131 Padova, Italy

*Corresponding author, E-mail: A.G.: armando.gennaro@unipd.it

P. L.: pengliu@pitt.edu

K. M.: km3b@andrew.cmu.edu.

Table of Contents

General remarks

Materials.

Ethyl α-bromophenylacetate, ethyl α-bromoisobutyrate, ethyl α-chlorophenylacetate, methyl methacrylate, 10-methylphenothiazine, phenothiazine, 2,3-dihydroxynaphthalene, 2-aminothiophenol, 9-phenylcarbozole, thianthrene, 9,10-bis[(triisopropylsilyl)ethynyl]-anthracene, 4,4'-bis(*N*-carbazolyl)-1,1'-biphenyl, chlorobenzene (anhydrous), RuPhos (2-dcyclohexylphosphino-2',6'-diisopropoxybiphenyl), RuPhos Pd G2 (chloro(2-dicyclohexylphosphino-2',6'-diisopropoxy-1,1'-biphenyl)[2-(2'-amino-1,1'-biphenyl)]-palladium(II)), 4-bromoanisole, 1-chloronaphthalene, 2-chloropyridine, dioxane, MeCN, DMF and DMA were purchased from Aldrich. Methyl methacrylate was purified by passing through a column of basic alumina to remove the inhibitor. All solvents and chemicals were used as received, unless described in detail below.

Instrumentation.

^{1}H nuclear magnetic resonance (NMR) measurements were performed on a Bruker Avance 300 MHz spectrometer. Molecular weight (MW) and molecular weight distribution (MWD, M_w/M_n values) were determined by gel permeation chromatography (GPC). The GPC system used a Waters 515 HPLC pump and a Waters 2414 refractive index detector using PSS columns (Styrogel 10^2, 10^3, 10^5 Å) with THF as the eluent at a flow rate of 1 mL/min at 35 °C using a linear PMMA standard. Prior to analysis the sample was diluted with THF and filtered through a column of neutral alumina to remove the catalyst, and then filtered through a 0.2 μm poly(tetrafluoroethylene) (PTFE) membrane filter before injecting into GPC columns (inject volume: 40 μL) with toluene

as the flow marker. All the photoinduced ATRPs were conducted with one of two photoreactors: a 2.1 mW/cm^2 SHANY® UV (http://www.shanycosmetics.com/) or a 4.9 mW/cm^2 MelodySusie® UV (http://www.melodysusie.com/).

Cyclic voltammetry (CV) analyses of the photoactivators were conducted in DMA + 0.1 M *n*-Bu_4NClO_4 (Alfa Aesar, Electrochemical grade). CV traces were recorded on a Gamry Reference 600 potentiostat using a three electrode cell with a Pt disk working electrode (diameter = 3 mm, Gamry), which was cleaned by polishing with a 0.25 μm diamond paste and rinsed in an ultrasound bath for 5 minutes prior to each analysis. The counter electrode was a Pt wire, and the reference electrode was Ag|AgI|0.1 M n-Bu_4NI in DMF. The latter was calibrated after each experiment against the ferrocenium/ferrocene couple (Fc^+/Fc), which allowed conversion of all potentials to the aqueous saturated calomel electrode (SCE) scale by using $E°_{Fc^+/Fc}$ = 0.527 V vs. SCE in DMA. The working solution was degassed with N_2 for 15 min and then kept under a positive N_2 pressure.

FLP measurements were carried out by excitation with a 375 nm pulsed diode laser (LDH-PC-375, PicoQuant), and the decays were recorded using time-correlated single photon counting electronics (PicoHarp300, Picoquant). The absorption and emission and excitation spectra of the catalysts (0.7 mM) were obtained using a Cary 50 UV-visible spectrophotometer and a FluoroMax-2 Jobin Yvon SPEX spectrofluorometer, respectively.

Experimental procedures

General procedure for synthesis of N-aryl phenothiazine catalysts:

NaOtBu (134 mg, 1.4 mmol), phenothiazine (199 mg, 1 mmol), RuPhos Precat (14 mg, 0.02 mmol, 2 mol %), and RuPhos (8 mg, 0.02 mmol, 2 mol %) were added to a vial armed with a magnetic stir bar. The vial was evacuated and refilled with nitrogen three times before adding dry dioxane (1 mL) followed by addition of the aryl halide (1.4 mmol). The vial was placed in an oil bath at 110 °C with stirring for 6 h. The vial was then cooled to room temperature, diluted with CH_2Cl_2, washed with water, brine, dried with Mg_2SO_4, and purified using column chromatography. The products were dried under reduced pressure. 10*H*-Phenylphenothiazine (Ph-PTZ, **2**), 4-methoxyphenyl-10*H*-phenothiazine (MeOPh-PTZ, **4**), and 1-naphthalene-10*H*-phenothiazine (Nap-PTZ, **7**) were synthesized using the described procedure and their spectral data matched those previously reported.[1]

4-Chloro-10*H*-phenothiazine (ClPh-PTZ, **5**): yellowish solid, ^{1}H NMR (300 MHz, $CDCl_3$) δ**:** 7.59-7.55 (2H, m), 7.36-7.32 (2H, m), 7.07-7.04 (2H, m), 6.93-6.83 (4H, m), 6.27-6.23 (2H, m) ppm.

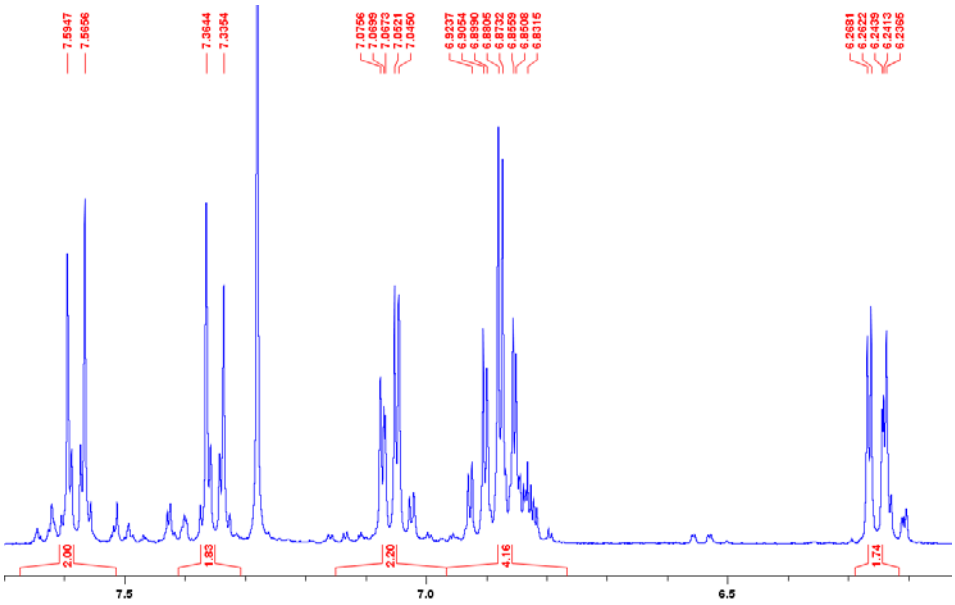

Figure S1. ^{1}H NMR spectrum of compound **5**, ClPh-PTZ.

10-(Pyridin-2-yl)-10*H*-phenothiazine (2-Py-PTZ, **6**): yellowish solid, ^{1}H NMR (300 MHz, $CDCl_3$) δ**:** 8.30 (1H, dd, *J* = 4.9, 1.1 Hz), 7.58 (2H, dd, *J* = 8.0, 1.0 Hz), 7.53-7.46 (1H, m), 7.40 (2H, dd, *J* = 7.7, 1.2 Hz), 7.32-7.27 (2H, m), 7.16 (2H, td, J = 7.6, 1.2 Hz), 6.94 (1H, d, *J* = 8.5 Hz), 6.91-6.86 (1H, m) ppm.

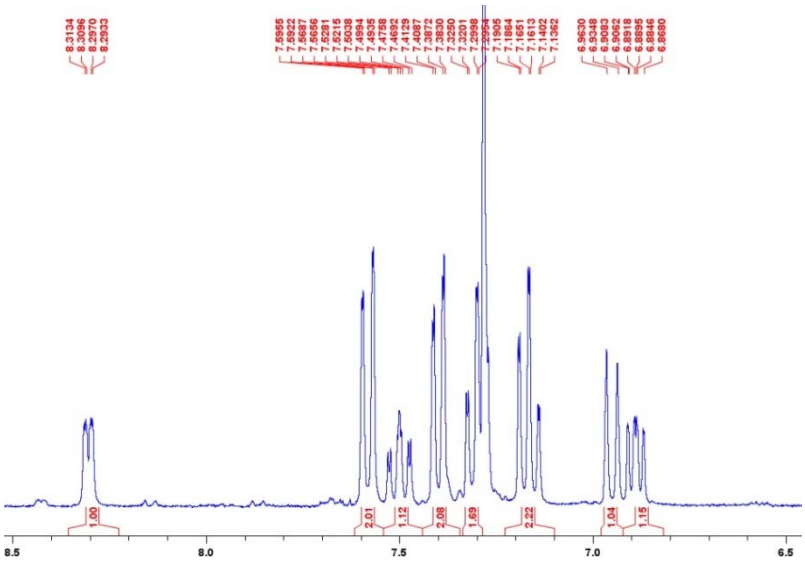

Figure S2. ^{1}H NMR spectrum of compound **6**, Py-PTZ.

General procedure for synthesis of benzo[b]phenothiazine:[2]

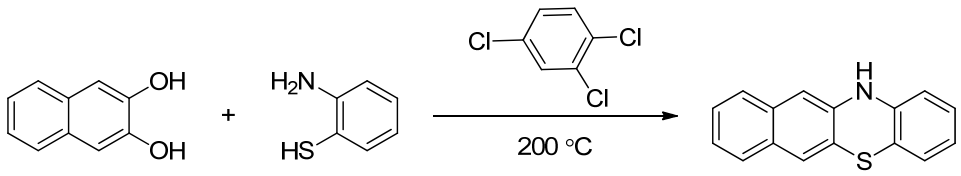

A mixture of 8 g (0.05 mol) of 2,3-dihydroxynaphthalene, 6.25 g (0.05 mol) of 2-aminothiophenol and 25 mL of 1,2,4-trichlorobenzene (bp 215 °C) were placed in a 50 mL round bottom flask fitted with a magnetic stirrer and a vapor trap. Using a sand bath, the reaction mixture was heated to 200 °C and maintained at that temperature for 6 h. During that time, water was formed and collected in the trap. On cooling, the product crystallized from the reaction mixture. The product mixture was diluted with n-hexane and the yellow crystalline benzo[*b*]phenothiazine was collected by filtration and washed with fresh n-hexane and then ethanol. The product benzo[*b*]phenothiazine was obtained as yellow powder: ^{1}H NMR (300 MHz, $CDCl_3$) δ: 7.54 (2H, t, J = 8.4 Hz), 7.45 (1 H, s), 7.34-7.19 (2H, m), 7.03 (2H, t, J = 7.5 Hz), 6.87-6.80 (2H, m), 6.61 (1H, d, J = 7.8 Hz), 6.09 (1H, br s) ppm.

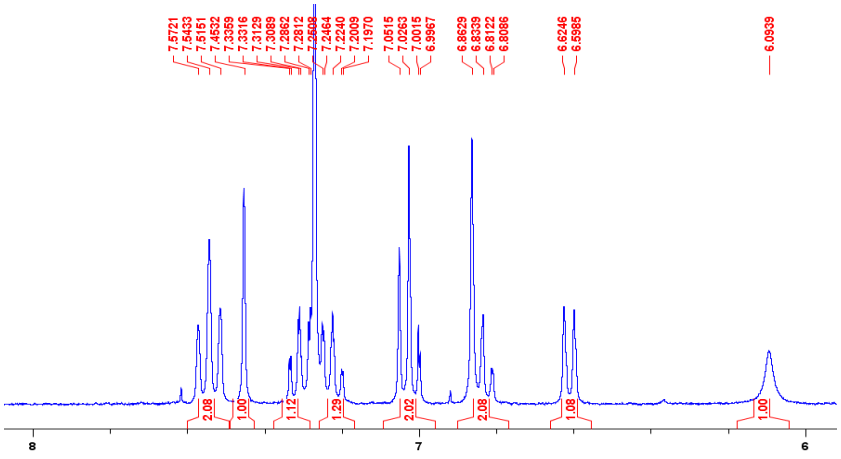

Figure S3. ^{1}H NMR spectrum of benzo[*b*]phenothiazine.

General procedure for synthesis of phenyl-benzo[b]phenothiazine, 10:

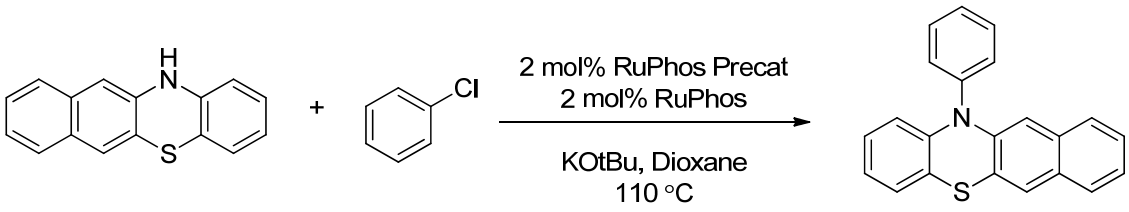

NaOtBu (268 mg, 2.8 mmol), benzo[*b*]phenothiazine (498 mg, 2 mmol), RuPhos Precat (28 mg, 0.04 mmol, 2 mol %), and RuPhos (16 mg, 0.04 mmol, 2 mol %) were added to a round bottom flask fitted with a magnetic stir bar. The vial was evacuated and backfilled with nitrogen gas three times before adding dry dioxane (2 mL) and then anhydrous chlorobenzene (286 microL, 2.8 mmol). The vial was then placed in an oil bath at 110 °C and stirred for 6 h. The vial was then cooled to room temperature, diluted with CH_2Cl_2 and the solution washed with water, brine, dried with Mg_2SO_4, and purified using column chromatography. After chromatography, the product was obtained as a yellow solid: ^{1}H NMR (300 MHz, $CDCl_3$) δ: 7.68 (2H, t, *J* = 7.5 Hz), 7.59-7.52 (2H, m), 7.47-7.44 (2H, m), 7.37-7.31 (2H, m), 7.22-7.19 (2H, m), 7.07 (1H, dd, J = 7.2, 1.7 Hz), 6.90-6.78 (2H, m), 6.38 (1H, s), 6.21-6.18 (1H, m) ppm.

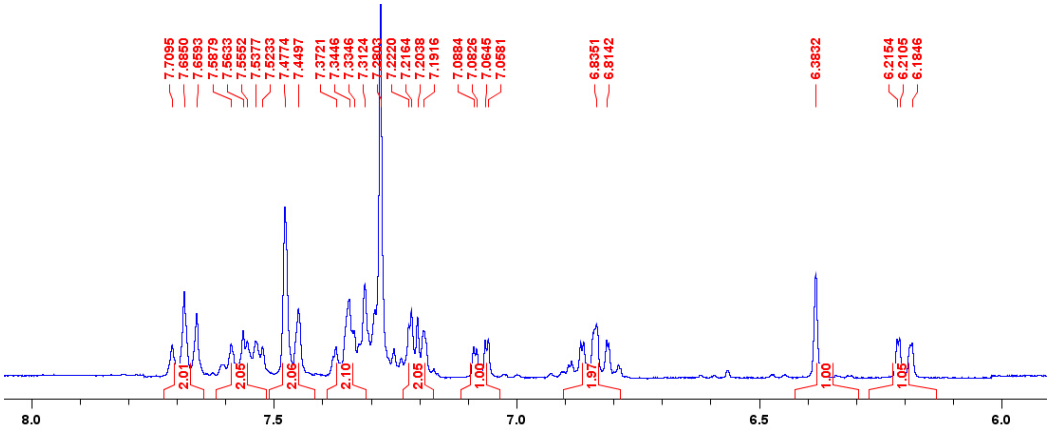

Figure S4. ^{1}H NMR spectrum of compound **10**, Ph-benzoPTZ.

General procedure for photoinduced metal-free ATRP:

Methyl methacrylate (2.1 mL, 20 mmol, 100 equiv), 0.035 mL of ethyl α-bromophenylacetate (EBPA, 48.6 mg, 0.2 mmol, 1 equiv), 5.5 mg of Ph-PTZ (**2**, 0.02 mmol, 0.1 equiv), and 2.1 mL of DMA were added into a 10 mL Schlenk flask. The flask was tightly sealed and oxygen was removed by three cycles of freeze-pump-thaw. The reaction mixture was irradiated by either 2.1 or 4.9 mW/cm^2 UV light. Samples were removed from the reaction mixture periodically by syringe to obtain the conversion of MMA by ^{1}H NMR, and number-average molecular weight M_n, and dispersity (M_w/M_n) by GPC using THF as eluent and linear PMMA standards.

Additional experimental data

Salt effect: Br$^-$

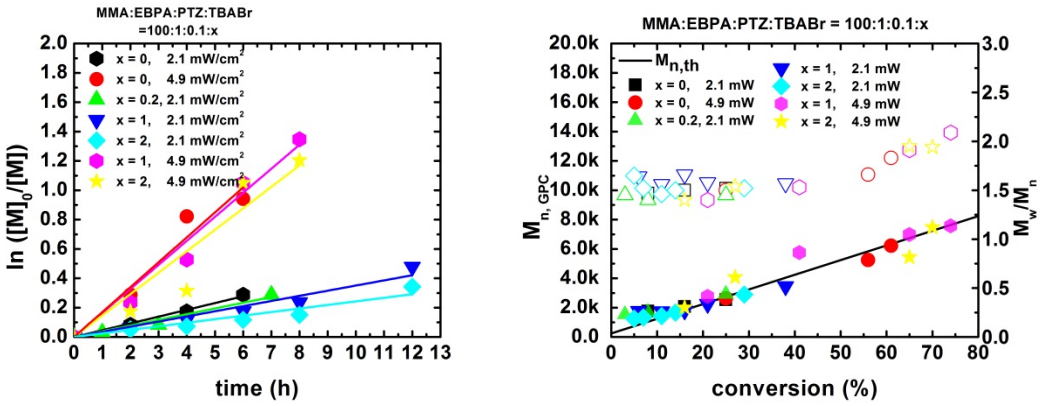

Figure S5. a) Left, semilogarithmic kinetic plots of polymerization of MMA with or without TBABr under conditions: $[MMA]_0:[EBPA]_0:[Ph\text{-}PTZ]_0:[TBABr]_0$ = 100:1:0.1:x, in MMA/DMA 1/1 (v/v), at room temperature with irradiation of 365 nm (2.1 or 4.9 mW/cm^2); b) right, number-average molecular weight (M_n, filled symbols), and dispersity (M_w/M_n, open symbols) versus conversion.

Salt effect: PF_6^-

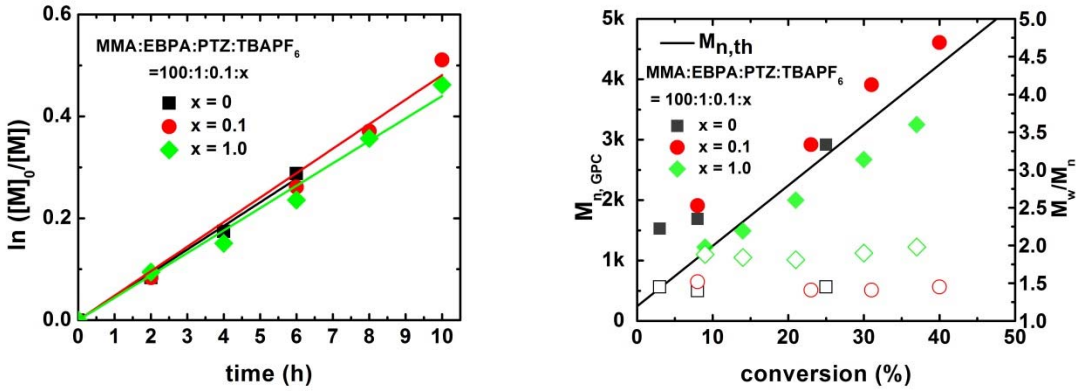

Figure S6. a) Left, semilogarithmic kinetic plots of polymerization of MMA with or without TBABr under conditions: $[MMA]_0:[EBPA]_0:[Ph\text{-}PTZ]_0:[TBAPF_6]_0 = 100:1:0.1:x$, in MMA/DMA 1/1 (v/v), at room temperature with irradiation of 365 nm (2.1 mW/cm^2); b) right, number-average molecular weight (M_n, filled symbols), and dispersity (M_w/M_n, open symbols) versus conversion.

Characterizations of all catalysts

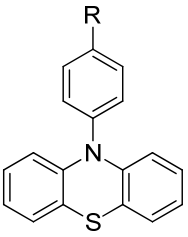

2, R = H, Ph-PTZ
4, R = OMe, MeOPh-PTZ
5, R = Cl, ClPh-PTZ

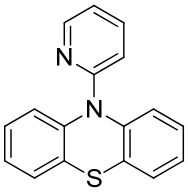

6, Py-PTZ

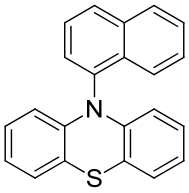

7, Nap-PTZ

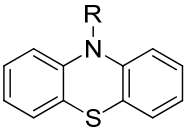

8, R = Me, Me-PTZ
9, R = H, H-PTZ

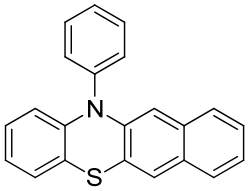

10, Ph-benzoPTZ

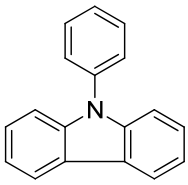

11, Ph-CBZ

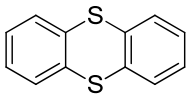

12, TH

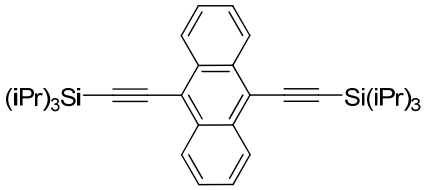

13, TIPS-AN

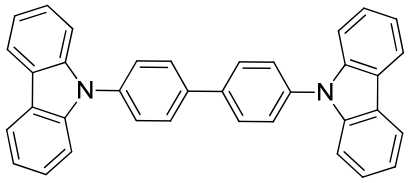

14, CBZ-Ph-Ph-CBZ

Emission and excitation spectra

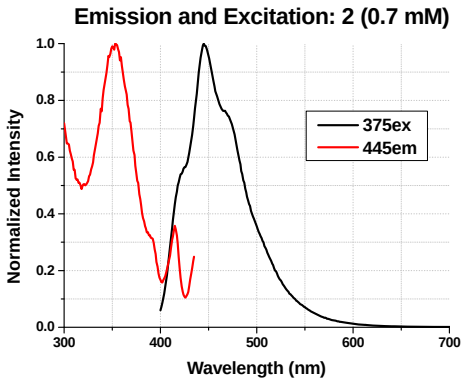

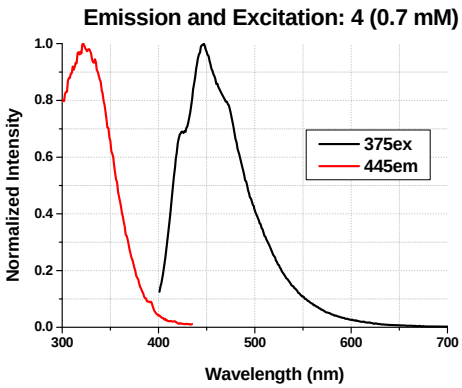

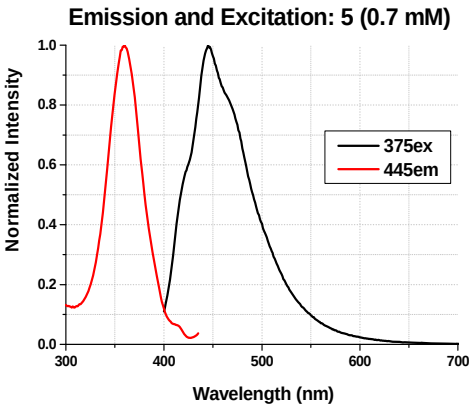
Emission and Excitation: 5 (0.7 mM)
Normalized Intensity
Wavelength (nm)
375ex
445em

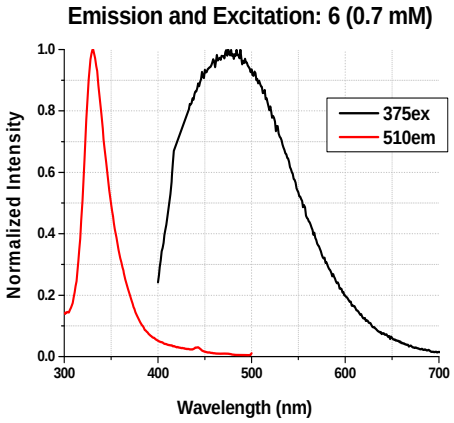
Emission and Excitation: 6 (0.7 mM)
Normalized Intensity
Wavelength (nm)
375ex
510em

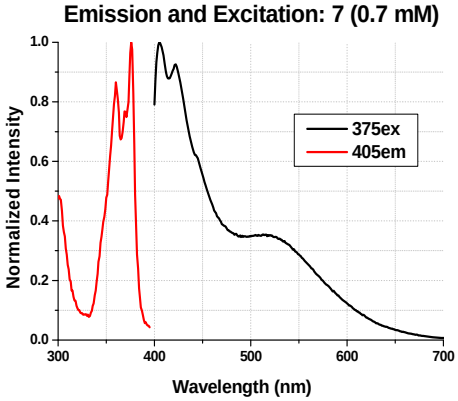
Emission and Excitation: 7 (0.7 mM)
Normalized Intensity
Wavelength (nm)
375ex
405em

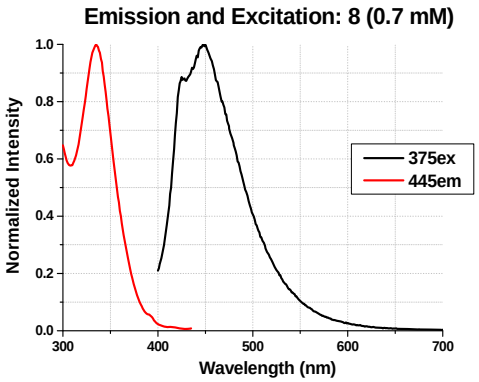
Emission and Excitation: 8 (0.7 mM)
Normalized Intensity
Wavelength (nm)
375ex
445em

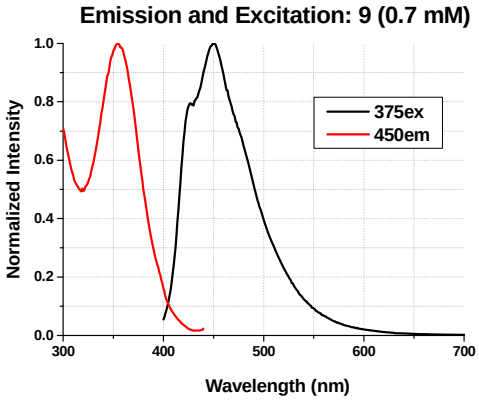
Emission and Excitation: 9 (0.7 mM)
Normalized Intensity
Wavelength (nm)
375ex
450em

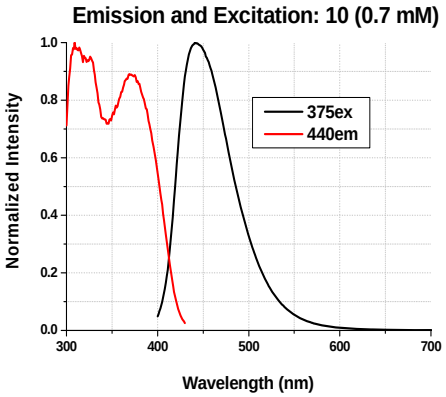
Emission and Excitation: 10 (0.7 mM)
Normalized Intensity
Wavelength (nm)
375ex
440em

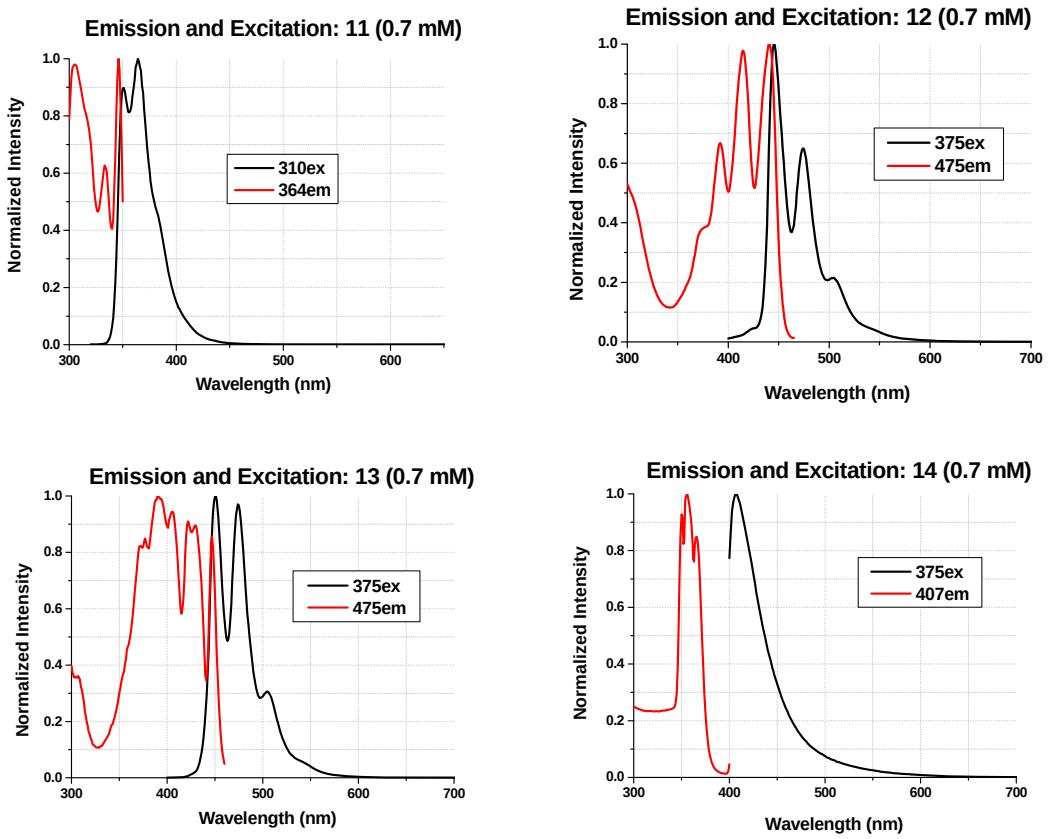

Figure S7. Emission and excitation spectra of catalysts. Concentration of all catalysts is 0.7 mM.

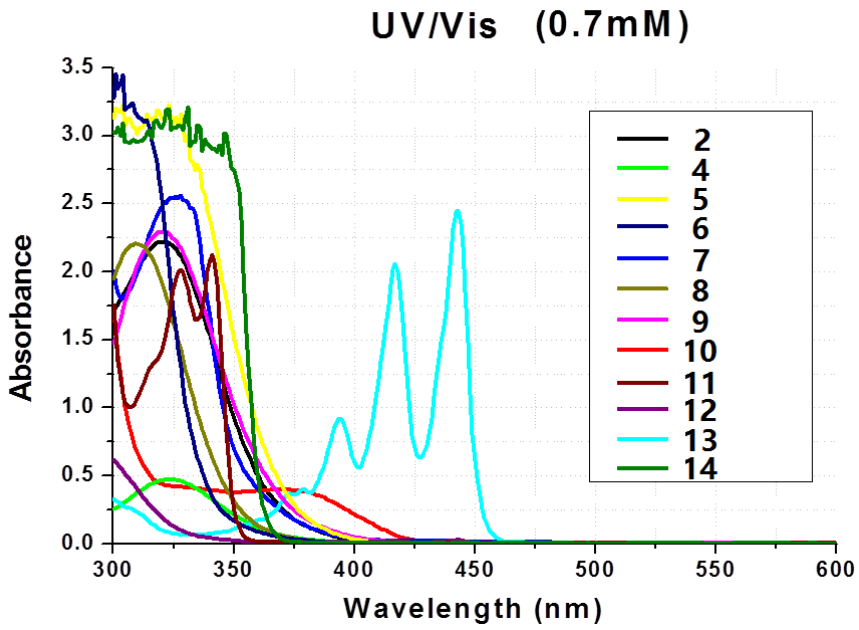

Figure S8. UV-vis spectra of catalysts shown in Figure 2. Concentration of all catalysts is 0.7 mM.

Cyclic voltammetry of 9, 11 and 12 at various scan rates

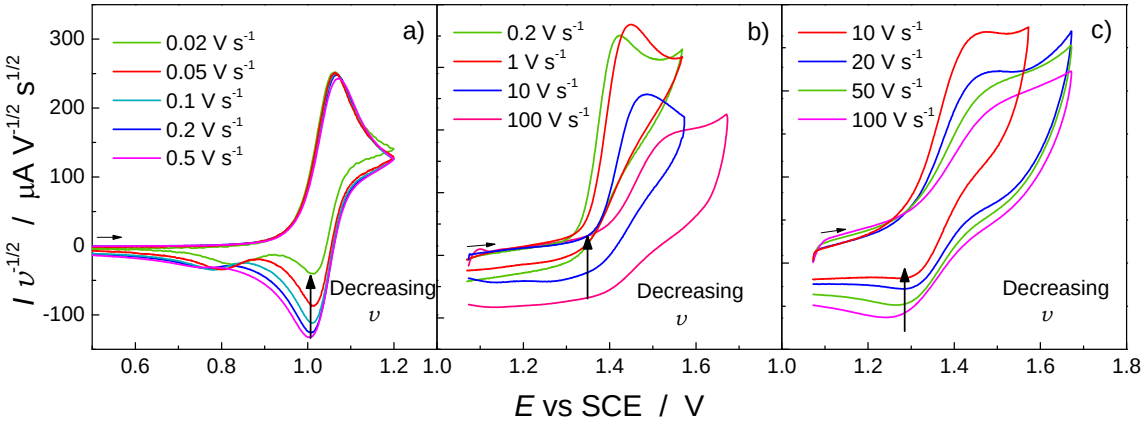

Figure S9. Cyclic voltammetry of 2×10^{-3} M a) **9**, b) **11** and c) **12** at various scan rates. Current intensity has been normalized by $\upsilon^{-1/2}$.

Oxidized phenothiazine **9** has limited chemical stability. The series of cyclic voltammograms in Figure S9 shows that as the scan rate is reduced, the cathodic current progressively decreases. This can be explained because at lower scan rates the radical cation has more time to decompose, generating a product that can be reduced at $E \approx 0.8$ V vs. SCE. In the CV conducted at 0.02 V s^{-1} roughly half of $\mathbf{9}^{\bullet+}$ has decomposed. At this slow scan rate, the reverse scan reaches the cathodic peak potential *ca* 8 s after potential inversion. Since in this time lapse *ca* 50% of $\mathbf{9}^{\bullet+}$ undergoes decomposition, the lifetime of the radical cation in DMA can be estimated to be *ca* 10 s. Also **12** shows a similar behavior with a faster decay rate, with a lifetime <5 ms. Other tested compounds (**11** and **14**) exhibited an irreversible oxidation peak for $\upsilon \leq 100$ V s^{-1}, indicating that their specific radical cations are not stable in DMA (lifetime < 10^{-3} s).

Polymerization with different catalysts

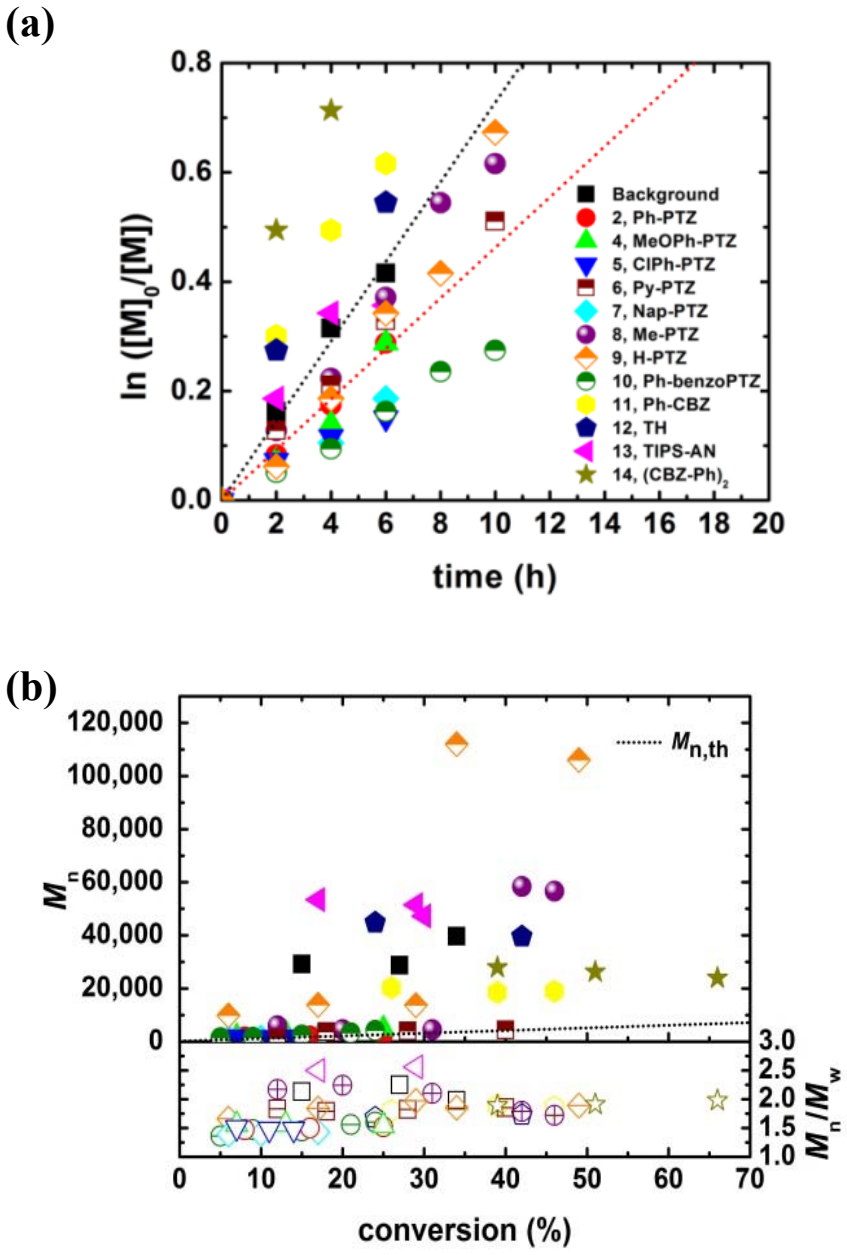

Figure S10. a) Semilogarithmic kinetic plots of polymerization of MMA with catalysts shown in Figure 3, conditions: $[MMA]_0:[EBPA]_0:[Cat]_0$ = 100:1:0.1, in MMA/DMA = 1/1 (v/v), at rt with 365 nm (2.1 mW/cm^2); b) M_n, (filled symbols), and dispersity (M_w/M_n, open symbols) versus conversion. Red dot line: linear fit for standard polymerization with **2**, black dot line: linear fit for background polymerization.

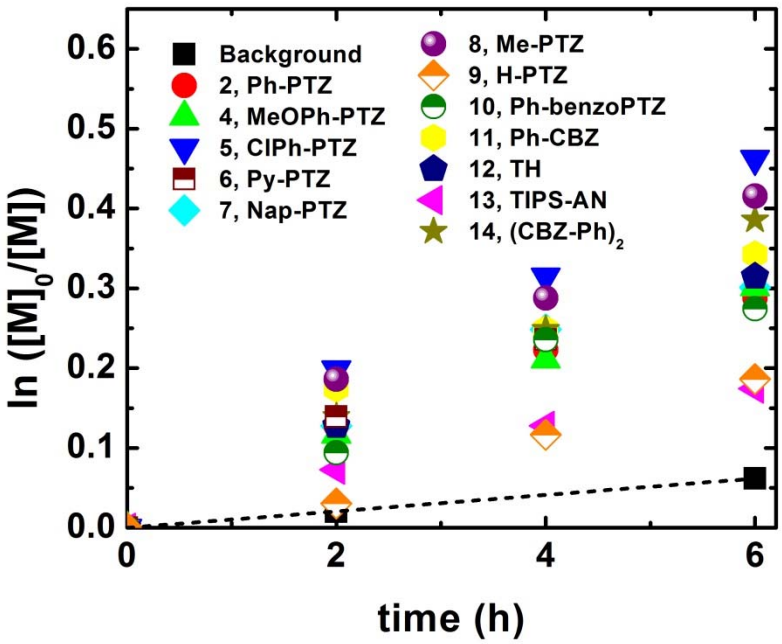

Figure S11. Semilogarithmic kinetic plots of polymerization of MMA with catalysts shown in Figure 3, conditions: $[MMA]_0:[EBiB]_0:[Cat]_0 = 100:1:0.1$, in MMA/DMA = 1/1 (v/v), at room temperature with irradiation of 365 nm (2.1 mW/cm^2); black line: linear fit for background polymerization.

Kinetic analysis of photoinduced ATRP activation

The reduction of MBiB by a series of electron donors (catalyst, Cat) was studied at 25 °C.

$$Cat + RX \xrightarrow{k_{act}} Cat^{\bullet+} + R^{\bullet} + X^{-} \qquad (1)$$

This reaction is an outer sphere electron transfer (OSET) from a donor (Cat) to an acceptor (RX), which undergoes a concerted bond breakage. It is a special case of outer sphere electron transfer, and it is known as dissociative electron transfer (DET).

In the following description of kinetic analysis all equations refer to the general activation reaction (1), but the numerical calculations will be illustrated taking the reaction of the catalyst Ph-PTZ* (**2***) with MBiB as an example. According to the sticky model of dissociative electron transfer theory,[3-6] the rate constant of reaction (1) can be calculated by

$$k_{\text{act}} = Z \exp\left(-\frac{\Delta G^{\ddagger}}{RT} \right) \qquad (2)$$

$$\Delta G^{\ddagger} = \Delta G_0^{\ddagger}\left(1 + \frac{\Delta_{\text{r}} G^{\ominus} - D_{\text{p}}}{4\Delta G_0^{\ddagger}} \right) \qquad (3)$$

$$\Delta G_0^{\ddagger} = \frac{\left(\sqrt{D_{\text{RX}}} - \sqrt{D_{\text{p}}}\right) + \lambda_{\text{o}}}{4} \qquad (4)$$

where $\Delta_{\text{r}}G^{\ominus}$ is the reaction free energy, $\Delta G_0^{\ddagger}$ is the intrinsic barrier (*i.e.* the activation free energy when $\Delta_{\text{r}}G^{\ominus} = 0$) of the reaction (1), λ_{o} is the solvent reorganization energy, D_{RX} is the R–X bond dissociation energy and D_{p} is the interaction energy between R$^{\bullet}$ and X^{-} in the solvent cage.

For activated alkyl bromides like MBiB, D_{p} is always small in polar solvents like DMF and CH_3CN, e.g. 0.24 – 0.50 kcal mol^{-1}.[7] The radical–anion interactions depend on the dielectric constant, which has very similar values for CH_3CN, DMF and DMA. The interaction energy between the methyl isobutyrate radical (MiB$^{\bullet}$) and X^{-} in DMA is not known. We used the value reported for the methyl propionate radical and X^{-} in CH_3CN

(0.24 and 0.69 kcal mol^{-1} for Br^- and Cl^-, respectively). The relevant thermodynamic, kinetic and geometric parameters used in the calculations are listed in Table S1.

Table S1. Thermodynamic, kinetic and geometric parameters for the homogenous electron transfer to RX.

Cat	RX	r_{Cat} Å	r_{RX} Å	r^a Å	λ_o kcal mol^{-1}	D_{RX} kcal mol^{-1}	$E^{\ominus}_{RX/R^{\bullet}+X^-}$ [b] V vs. SCE	D_P kcal mol^{-1}
1*, $Ir(ppy)_3$*	MBiB	5.31[c]	3.42	2.80	14.21	58.7	-0.52	0.24
2*, Ph-PTZ*	MBiB	4.49	3.42	2.80	14.53	58.7	-0.52	0.24
2*, Ph-PTZ*	EBPA	4.49	3.64	2.86	14.24	53.9	-0.22	0.24
2*, Ph-PTZ*	MCiB	4.49	3.47	2.68	15.07	75.7	-0.76	0.69
2, Ph-PTZ	MBiB	4.21	3.42	2.80	14.71	58.7	-0.52	0.24
8*, Me-PTZ*	MBiB	3.94	3.42	2.80	14.94	58.7	-0.52	0.24
11*, Ph-CBZ	MBiB	4.37	3.42	2.80	14.60	58.7	-0.52	0.24

Effective radius of DET products ($R^{\bullet}+X^-$) calculated as $r = (2r_{RX} - r_X)r_X / r_{RX}$. [b]Standard potential of the redox reaction $RX + e^- \longrightarrow R^{\bullet} + X^-$. [b]Calculated from crystallographic data.[8]

$\Delta_r G^{\ominus}$ of reaction (1) was calculated from the standard potentials of the donor and acceptor redox couples in the ground state, $E^{\ominus}_{Cat^{\bullet+}/Cat}$ and $E^{\ominus}_{RX/R^{\bullet},X^-}$, and the energy of the excited reactant, $E_{h\nu}$, using the Weller equation:[9]

$$\Delta_r G^{\ominus} = F\left(E^{\ominus}_{Cat^{\bullet+}/Cat} - E^{\ominus}_{RX/R^{\bullet}+X^-} - E_{h\nu}\right) - \frac{N_A e^2}{4\pi\varepsilon_0 \varepsilon r} \quad (5)$$

$$\Delta_r G^{\ominus} = 96485\,\mathrm{C\,mol^{-1}}(0.815 + 0.52 - 2.787)\mathrm{V} - \frac{6.022\times10^{23}\,\mathrm{mol^{-1}}(1.602\times10^{-19}\,\mathrm{C})^2}{4\times3.1416\times8.854\times10^{-12}\,\mathrm{J^{-1}C^2m^{-1}}\times37.78\times(4.49+3.42)\times10^{-10}\,\mathrm{m}}$$
$$= -144.7\,\mathrm{kJ\,mol^{-1}} = -34.59\,\mathrm{kcal\,mol^{-1}}$$

where e is the elementary charge, ε_0 is the permittivity of vacuum and ε the relative permittivity of the solvent at 25 °C.[10] The last term is the Coulombic energy experienced by the ions $Cat^{\bullet+}$ and X^- at a distance r (the distance was approximated to the sum of the radii of the two hitting molecules $r = r_{Cat*} + r_{RX}$). The radii were obtained from the computed volume of the molecules, based on an isoelectron density surface of 0.001 electrons/Bohr^3 using the DFT-optimized structures (see below for further details on the DFT optimizations).

$E^{\ominus}_{Cat^{\bullet+}/Cat}$ = and E_{hv} were experimentally determined in DMA (Table 3 in the main text). Values of $E^{\ominus}_{RX/R^{\bullet}+X^-}$ for MBiB and MCiB were taken from the literature,[11] whereas $E^{\ominus}_{RX/R^{\bullet}+X^-}$ of EBPA was calculated from published thermodynamic data[3] as described previously.[11]

The intrinsic barrier $\Delta G_0^{\ddagger}$ was calculated as

$$\Delta G_0^{\ddagger} = \frac{\left(\sqrt{D_{RX}} - \sqrt{D_p}\right) + \lambda_o}{4} = \frac{\left(\sqrt{58.7} - \sqrt{0.24}\right) + 14.53}{4}\,\mathrm{kcal\,mol^{-1}} = 16.49\,\mathrm{kcal\,mol^{-1}}$$

where D_{RX} is RX bond energy, obtained through DFT calculation.

The solvent reorganization energy λ_o was determined by using an empirical equation obtained on the basis of an extensive set of experimental data:[13,14]

$$\lambda_o = 95\left(\frac{1}{2r_{Cat}} + \frac{1}{2r} - \frac{1}{r_{Cat}+r}\right)\text{kcal mol}^{-1} = 14.53\,\text{kcal mol}^{-1} \qquad (7)$$

where r is the effective radius of RX, which was calculated from the equation $r = (2r_{RX} - r_X)r_X/r_{RX}$.[3,15] using r_{Br} = 1.96 Å, r_{Cl} = 1.81 Å[16] together with the r_{Cat} and r_{RX} values reported in Table S1.

***k*act estimate.** The rate constant of reaction (1) can be calculated as follows:

$$k_{act,DET} = Z\exp\left(-\frac{\Delta G^{\ddagger}}{RT}\right) \qquad (2)$$

$$Z = N_A\sqrt{\frac{8\pi RT}{\mu}}\left(r_{Cat}+r_{RX}\right)^2$$

In the case Cat = Ph-PTZ* (**2***) (M = 275.38 g mol^{-1}) and RX = MBiB (M = 181.03 g mol^{-1}), μ = 109.22 g mol^{-1} and Z = 2.85 10^{11} M^{-1} s^{-1}.

Using D_P = 0.24 kcal mol^{-1} for Br$^-$ and 0.69 kcal mol^{-1} for Cl$^-$, and calculating λ_o from eq. (7), $\Delta G_0^{\ddagger}$ was computed for all Cat/RX couples. The activation free energy of reaction (1) was then calculated through eq. (3). Finally, eq. (2) provided k_{act}. The results of all calculations are presented in Table 4 in the main text.

DFT Calculations

Computational Details

All DFT calculations were performed with the Gaussian 09 software package.[17] Geometries were optimized using the B3LYP functional and the 6-31G(d) basis set in solution. The SMD solvation model and DMF solvent were used in the calculations. Single point energies were calculated using M06-2X and 6-311++G(3df,2p) and the SMD solvation model in DMF. Reported Gibbs free energies and enthalpies in solution include thermal corrections computed at 298 K and are computed at the standard concentration (1 mol/L). The CCSD(T) benchmark calculations were performed with MOLPRO Version 2012.1.[18]

Benchmark calculations of the dissociation energy of $2^{\bullet+}Br^-$

To evaluate the accuracy of the computational method, we investigated the relative stabilities of **$2^{\bullet+}Br^-$-C** and **$2^{\bullet+}$** at different levels of theory (Table S2). DMF was used as the solvent in the SMD and CPCM solvation model calculations. The method used in this study, M06-2X/6-311++G(3df,2p), gives good agreement with the high-level DF-LCCSD(T)-F12/cc-pVTZ calculations in the gas phase (entries 6 vs. 8). Although the dissociation of the ion pair is highly unfavorable in the gas phase, the dissociation becomes slightly exergonic in solution. Calculations using the CPCM solvation model (entry 5) predicted the dissociation to be exergonic by 4.7 kcal mol^{-1}, while prediction of the SMD model is that dissociation is only slightly exergonic by 0.2 kcal/mol (entry 3). Using the experimental solvation free energy of bromide anion in DMF,[19] along with the solvation free energies computed with SMD for **$2^{\bullet+}Br^-$-C** and **$2^{\bullet+}$**, the calculations (entry 4) indicate that the dissociation of the ion pair is exergonic by 6.0 kcal/mol. These calculations suggest that the exact value of the ion pair dissociation energy in solution is challenging for computations, due to the relatively large errors in the solvation free energy calculations with the explicit solvation models. Based on the previous benchmark study by Cramer and Truhlar,[20] the average errors for SMD model for cations and anions in non-aqueous solutions are about 6 and 3 kcal mol^{-1}, respectively. The average errors for CPCM are greater than 10 kcal mol^{-1} for cations, and about 4 kcal mol^{-1} for anions. Considering these reported average errors, the SMD solvation model was used in the present study. It should be noted that the conclusions in this study will not be affected by the choice of the solvation model in the DFT calculations. Most importantly, the

termolecular pathway in deactivation is always the most favorable regardless of the solvation model used.

Table S2. The relative stabilities of $\mathbf{2^{\bullet+}Br^{-}\text{-}C}$ and $\mathbf{2^{\bullet+}}$ at different levels of theory.

$\mathbf{2^{\bullet+}Br^{-}\text{-}C \rightarrow 2^{\bullet+} + Br^{-}}$

		Dissociation energy (kcal mol^{-1})	
Entry	**Method**[a]	**ΔG**	**ΔH**
1	B3LYP/6-311G(3df,2p) (SMD)	-0.8	5.7
2	M06-2X/6-311G(3df,2p) (SMD)	2.3	8.8
3	M06-2X/6-311++G(3df,2p) (SMD)	-0.2	6.3
4	M06-2X/6-311++G(3df,2p) (SMD)[b]	-6.0	0.5
5	M06-2X/6-311++G(3df,2p) (CPCM)	-4.7	1.9
6	M06-2X/6-311++G(3df,2p) (gas)	83.3	89.8
7	DF-LUCCSD(T)/cc-pVDZ (gas)	87.5	94.0
8	DF-LUCCSD(T)/cc-pVTZ (gas)	82.3	88.9

[a]Method used in singlet point energy calculations. Geometries were optimized with B3LYP/6-31G(d) with the SMD solvation model in DMF for all calculations. Thermal corrections to *G* and *H* at 298 K were calculated using the same level of theory as in geometry optimization. [b] Experimental solvation free energy of bromide anion in DMF ($\Delta G_{s(Br-)} = -59.9$ kcal mol^{-1}) was used in place of the value computed by the SMD solvation model ($\Delta G_{s(Br-)} = -54.1$ kcal mol^{-1}). See ref.19.

Optimized geometries and molecular orbitals of Cat$^{\bullet+}$X^{-}

The optimized geometries, spin densities, NPA charges, and HOMO of the four **Cat$^{\bullet+}$X^{-}** complexes are shown below. Both the covalent and ionic isomers were taken into account. Energies are with respect to the dissociated radical cation **Cat$^{\bullet+}$** and the halide anion **X^{-}**. Relatively weak interactions between the catalyst radical cation and the halide anion are observed in all isomers.

2$^{\bullet+}$-Br-C

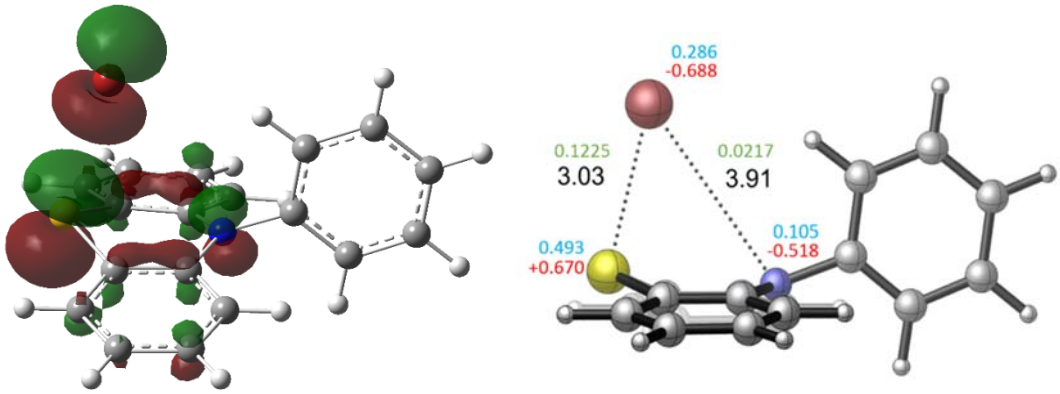

ΔG = -0.2 kcal/mol
ΔH = -7.2 kcal/mol

2$^{\bullet+}$-Br-I

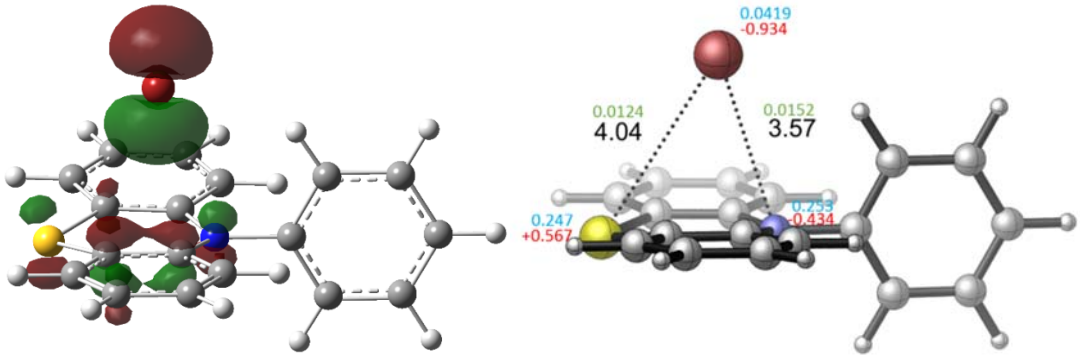

ΔG = 0.2 kcal/mol
ΔH = -6.3 kcal/mol

8*•+*-Br-C

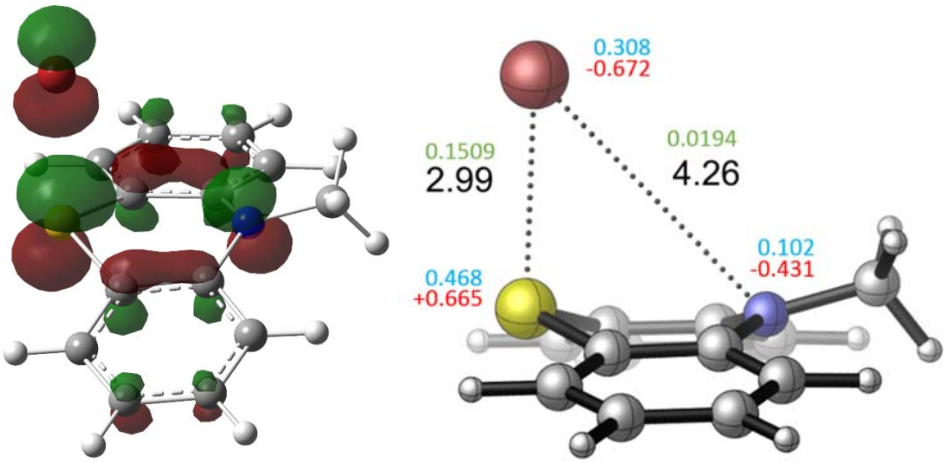

ΔG = -0.7 kcal/mol
ΔH = -7.2 kcal/mol

8*•+*-Br-I

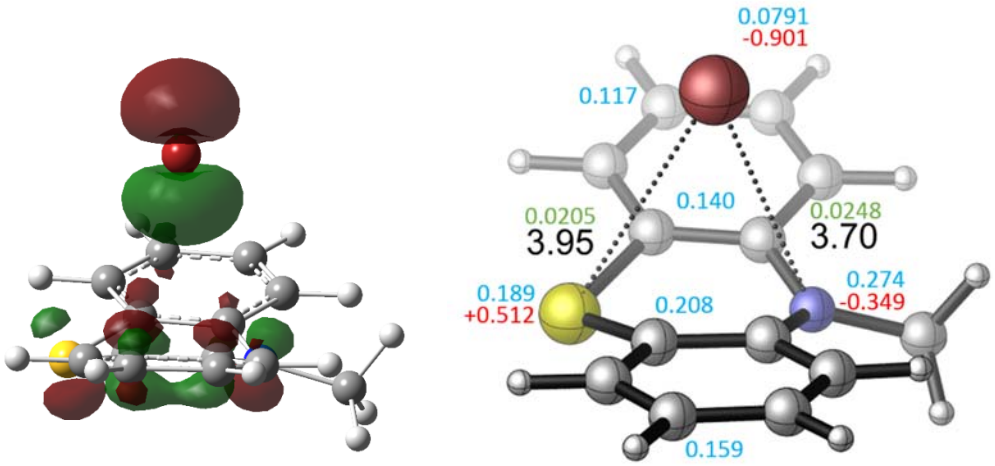

ΔG = 0.0 kcal/mol
ΔH = -6.5 kcal/mol

2*•+*-Cl-C

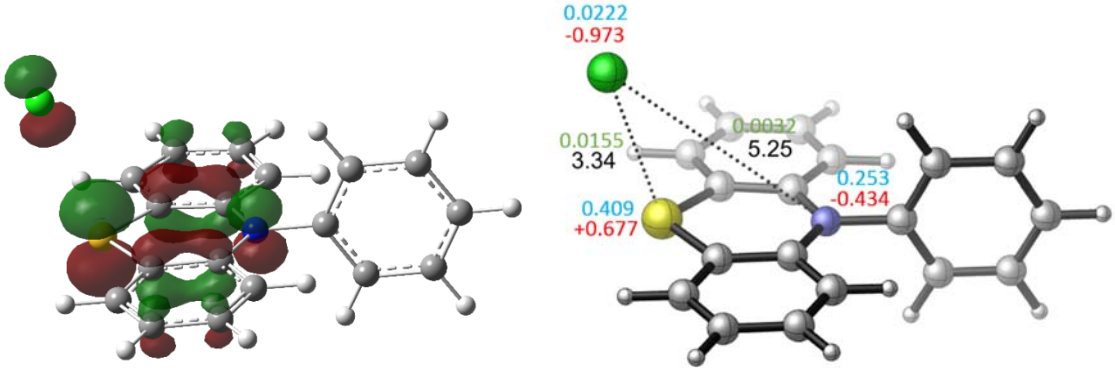

ΔG = 1.1 kcal/mol
ΔH = -3.8 kcal/mol

2*$^{\bullet+}$*-Cl-I

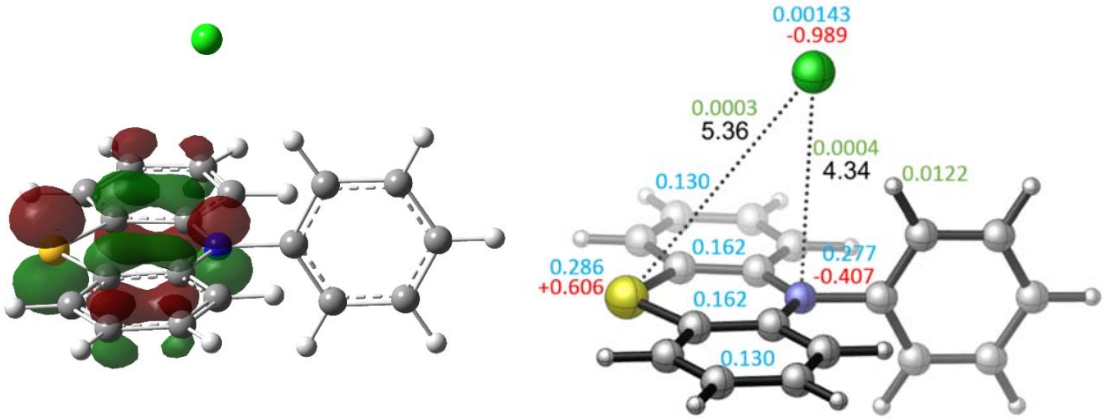

ΔG = 0.7 kcal/mol
ΔH = -4.6 kcal/mol

11*$^{\bullet+}$*-Br

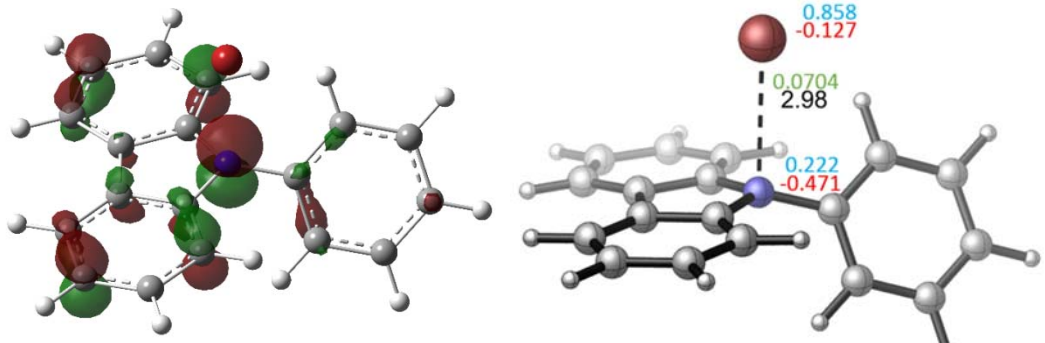

ΔG = -0.8 kcal/mol
ΔH = -7.5 kcal/mol

Figure S12. HOMO, spin densities (in blue), NPA charges (in red), and Wiberg bond indices (in green) of **Cat**$^{\bullet+}$**X**$^{-}$. Bond distances are shown in black.

Calculation of $E^{\ominus}_{MiB^+/MiB^\bullet}$ and $E^{\ominus}_{11^{\bullet+}/11}$

The computed free Gibbs energy of the reaction

$$\mathbf{2}^{\bullet+} + MiB^\bullet \rightleftarrows \mathbf{2} + MiB^+$$

is 8.6 kcal mol^{-1}. Therefore

$$-F(E^{\ominus}_{\mathbf{2}^{\bullet+}/\mathbf{2}} - E^{\ominus}_{MiB^+/MiB^\bullet}) = -F(0.815 - E^{\ominus}_{MiB^+/MiB^\bullet}) = \Delta_r G^{\ominus} = 8.6 \text{ kcal mol}^{-1} = 36.0 \text{ kJ mol}^{-1}$$

from which $E^{\ominus}_{MiB/MiB^\bullet}$ = 1.188 V vs. SCE is obtained.

Similarly, from $\Delta_r G^{\ominus}$ = -7.4 kcal mol^{-1} for the reaction

$$\mathbf{11}^{\bullet+} + MiB^\bullet \rightleftarrows \mathbf{11} + MiB^+$$

it is possible to obtain

$$-F(E^{\ominus}_{\mathbf{11}^{\bullet+}/\mathbf{11}} - E^{\ominus}_{MiB^+/MiB^\bullet}) = -F(E^{\ominus}_{\mathbf{11}^{\bullet+}/\mathbf{11}} - 1.188) = \Delta_r G^{\ominus} = -7.4 \text{ kcal mol}^{-1} = -31.0 \text{ kJ mol}^{-1}$$

and therefore $E^{\ominus}_{\mathbf{11}^{\bullet+}/\mathbf{11}}$ = 1.509 V vs. SCE.

$E^{\ominus}_{\mathbf{11}^{\bullet+}/\mathbf{11}}$ is more positive than the oxidation peak potential of **11** (E_p = 1.423 V vs. SCE at υ = 0.2 V s^{-1}). This was expected because **11** undergoes a quick reaction after the electron transfer (**11**$^{\bullet+}$ is highly unstable and quickly decomposes).

Examples of calculations of activation energies for deactivation pathways

Five possibilities were considered for the deactivation process: (a) inner-sphere electron transfer (ISET) mechanism; (b) dissociative electron transfer (DET); (c) outer-sphere electron transfer between $Cat^{\bullet+}X^-$ and $R^\bullet$ (OSET-I), followed by addition of X^- to R^+; (d) outer-sphere electron transfer between $Cat^{\bullet+}$ and $R^\bullet$ (OSET-II), followed by recombination of R^+ and X^-; (e) the termolecular associative electron transfer (AET-ter). Geometric and thermodynamic parameters for the three catalysts **2**, **8** and **11** and for the initiators MBiB and MCiB are provided in Table S3. Detailed calculations are here reported for the **2** + MBiB catalytic system, while results for all investigated systems are presented in Table 6 in the manuscript.

Table S3. Parameters used for the determination of energy barriers for the deactivation pathways.

Catalyst Complex	D_{RX} (kcal mol^{-1})	Radius (Å)			$\Delta_r G^\ddagger$ (kcal mol^{-1})		
		$MiB^\bullet$	$Cat^{\bullet+}$-X^-	$Cat^{\bullet+}$	OSET-I	OSET-II	DET
$2^{\bullet+}Br^-$	20.9	3.0	4.6	4.1	13.6	8.7	8.4
$2^{\bullet+}Cl^-$	36.0	3.0	4.5	4.1	11.0	8.7	7.5
$8^{\bullet+}Br^-$	20.1	3.0	4.0	4.0	11.3	7.5	8.2
$11^{\bullet+}Br^-$	6.8	3.0	4.1	4.4	-3.5	-7.4	-6.6

AET-ter deactivation

The exact reverse process of metal-free ATRP activation, which is a dissociative electron transfer (DET), is an associative electron transfer involving a termolecular encounter (AET-ter):

$$\mathbf{2} + \mathrm{RX} \underset{k_{\text{AET-ter}}}{\overset{k_{\text{act}}}{\rightleftarrows}} \mathbf{2}^{\bullet+} + \mathrm{X}^{-} + \mathrm{R}^{\bullet}$$

The activation free energy of the termolecular deactivation ($\Delta G^{\ddagger}_{\text{AET}-\text{ter}}$) is

$$\Delta G^{\ddagger}_{\text{AET-ter}} = \Delta G^{\ddagger}_{0}\left(1 - \frac{\Delta G^{\ominus} + D_{\text{p}}}{4\Delta G^{\ddagger}_{0}}\right)^{2}$$

In the case RX = MBiB with **2** as the photocatalyst, $\Delta G^{\ddagger}_{0} = 16.5\,\text{kcal mol}^{-1}$ and the DFT-calculated reaction free energy is $\Delta_{\text{r}}G^{\ominus}$ = 33.6 kcal mol^{-1}. In addition, D_{p} = 0.24 kcal mol^{-1}. Therefore, calculation of the activation free energy gives $\Delta G^{\ddagger}_{\text{AET}-\text{ter}} = 3.9\,\text{kcal mol}^{-1}$ as reported in Fig. 9 (main text).

When instead $\Delta_{\text{r}}G^{\ominus}$ = 29.6 kcal mol^{-1}, obtained from experimental data, was used together with the above $\Delta G^{\ddagger}_{0}$ and D_{p} values, a slight increase of $\Delta G^{\ddagger}_{\text{AET}-\text{ter}}$ to 5.0 kcal mol^{-1} was observed.

OSET-II deactivation

$$\mathbf{2}^{\bullet+} + \mathrm{R}^{\bullet} \rightleftarrows \mathbf{2} + \mathrm{R}^{+}$$

In this case, no bond is being breaken or formed during electron transfer, therefore:

$$\Delta G^{\ddagger}_{\text{OSET-II}} = \Delta G^{\ddagger}_{0}\left(1 + \frac{\Delta_{\text{r}}G^{\ominus}}{4\Delta G^{\ddagger}_{0}}\right)^{2}$$

$\Delta_r G^{\ominus}$ = 8.6 kcal mol^{-1} from DFT optimizations and $\Delta G_0^{\ddagger} = (\lambda_i + \lambda_o)/4$. The inner reorganization energy, λ_i, is fairly negligible for phenothiazines. This was observed by comparing the experimental barrier and the solvent reorganization energy of a series of phenothiazines (H-PTZ, Me-PTZ, [21] Bz-PTZ[22]). The rate constant of self-exchange, k_{ex}, is reported for a series of phenothiazines. The intrinsic barrier calculated is equal to $\lambda_o/4$ within the experimental error, indicating that these compounds do not undergo appreciable internal rearrangement upon ET. Therefore, λ_i can be fairly neglected. It is also likely that there are no significant structural changes on passing from R$^{\bullet}$ to R$^+$, since both molecules have sp^2 hybridization. Therefore, neglecting λ_i contribution in the intrinsic barrier and calculating the solvent reorganization energy as follows

$$\lambda_o = 95[(2r_{\mathbf{2}^{\bullet+}})^{-1} + (2r_{R\cdot})^{-1} - (r_{\mathbf{2}^{\bullet+}} + r_{R\cdot})^{-1}] = 95\left(\frac{1}{2\cdot 4.08} + \frac{1}{2\cdot 2.95} - \frac{1}{4.08+2.95}\right) = 14.23 \text{ kcal mol}^{-1}$$

lead to $\Delta G_0^{\ddagger} = 3.56 \text{ kcal mol}^{-1}$ and

$$\Delta G^{\ddagger}_{\text{OSET-II}} = (3.56 \text{ kcal mol}^{-1})\left(1 + \frac{8.6}{4\times 3.56}\right)^2 = 9.16 \text{ kcal mol}^{-1}$$

OSET-I deactivation

$\mathbf{2}^{\bullet+}$Br$^-$-C + R$^{\bullet}$ $\rightleftarrows$ **2**-Br$^-$-C + R$^+$

As in the case of OSET-II, Marcus theory of outer-sphere electron transfer can be applied to the OSET-T deactivation pathway:

$$\Delta G^{\ddagger}_{\text{OSET-I}} = \Delta G_0^{\ddagger}\left(1 + \frac{\Delta_r G^{\ominus}}{4\Delta G_0^{\ddagger}}\right)^2$$

$\Delta_r G^{\ominus}$ = 13.6 kcal mol^{-1} from DFT optimizations and, neglecting λ_i as in the case of OSET-II mechanism, gives $\Delta G_0^{\ddagger} = 3.47 \text{ kcal mol}^{-1}$ with λ_o given by

$$\lambda_o = 95[(2r_{Cat})^{-1} + (2r_{R\cdot})^{-1} - (r_{Cat} + r_{R\cdot})^{-1}] = 95\left(\frac{1}{2\cdot 4.56} + \frac{1}{2\cdot 2.95} - \frac{1}{4.56+2.95}\right) = 13.87 \text{ kcal mol}^{-1}$$

With these values $\Delta G^{\ddagger}_{\text{OSET-I}}$ is calculated as

$$\Delta G^{\ddagger}_{\text{OSET-I}} = \left(3.47 \text{ kcal mol}^{-1}\right)\left(1 + \frac{13.66}{4\times 3.47}\right)^2 = 13.6 \text{ kcal mol}^{-1}$$

DET deactivation

2$^{\bullet+}$Br$^-$-C + R$^\bullet$ → **2** + Br$^-$ + R$^+$

Sticky interaction does not occur here, because there is no interaction between Br$^-$ and a radical. The activation Gibbs free energy is therefore given by

$$\Delta G^{\ddagger}_{\text{DET}} = \Delta G^{\ddagger}_0\left(1 + \frac{\Delta_r G^{\ominus}}{4\Delta G^{\ddagger}_0}\right)^2$$

$\Delta_r G^{\ominus}$ = 8.4 kcal mol^{-1} from DFT optimizations, whereas $\Delta G^{\ddagger}_0$ for a dissociative electron transfer can be calculated from the bond dissociation energy and solvent reorganization energy:

$$\Delta G^{\ddagger}_0 = \frac{D_{\mathbf{2}^{\bullet+}\text{Br}^-\text{-C}} + \lambda_o}{4}$$

Using the computed $D_{\mathbf{2}^{\bullet+}\text{Br}^-\text{-C}}$ value of 6.3 kcal mol^{-1} and λ_o calculated as

$$\lambda_o = 95[(2r_{Cat})^{-1} + (2r_{R\cdot})^{-1} - (r_{Cat} + r_{R\cdot})^{-1}] = 95\left(\frac{1}{2\cdot 4.56} + \frac{1}{2\cdot 2.95} - \frac{1}{4.56+2.95}\right) = 13.87 \text{ kcal mol}^{-1}$$

leads to

$$\Delta G^{\ddagger}_{\text{DET}} = \left(5.04 \text{ kcal mol}^{-1}\right)\left(1 + \frac{13.6}{4\times 5.04}\right)^2 = 14.13 \text{ kcal mol}^{-1}$$

Energy profile of the deactivation in the reaction of 11•+Br− and MiB•

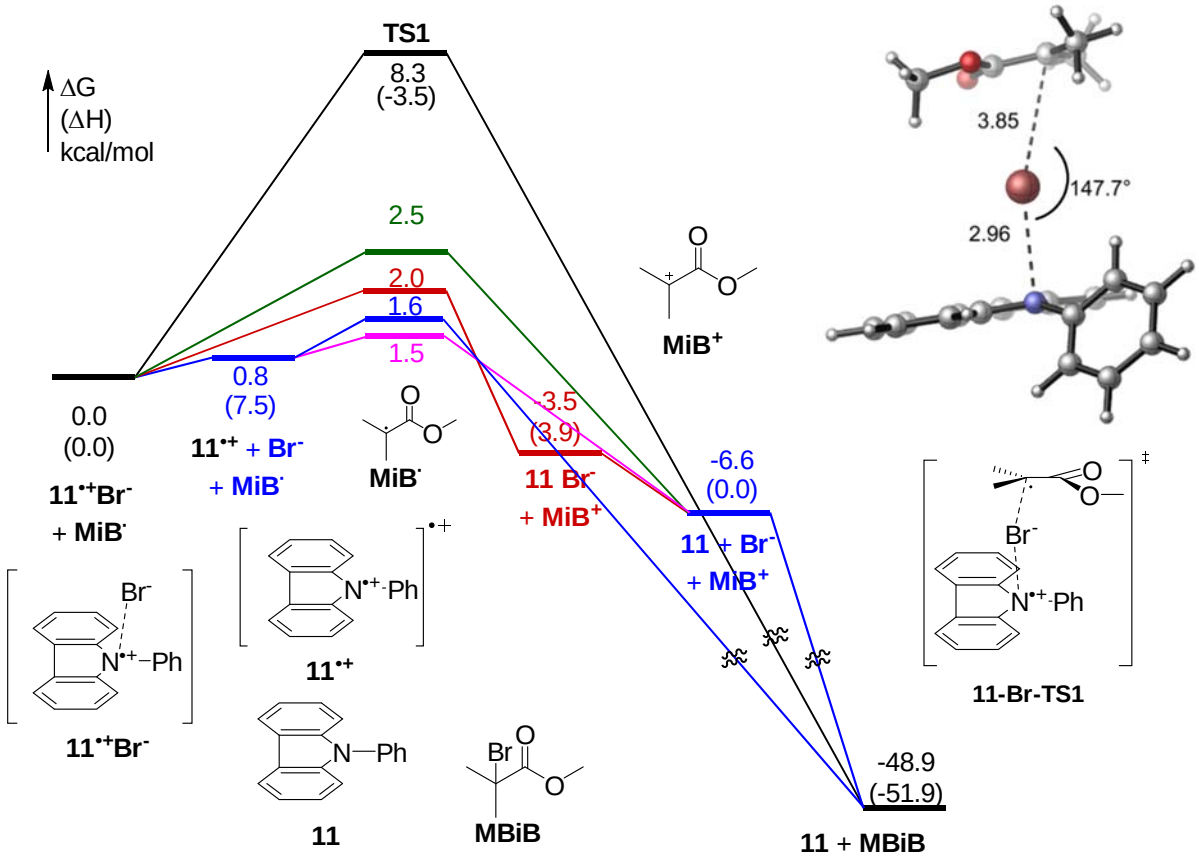

Figure S13. Computed reaction energy profiles for all deactivation pathways of MiB• by **11•+Br−**. Black: inner-sphere electron transfer (ISET) (*i.e.* concerted atom transfer); Green: dissociative electron transfer from MiB• to **11•+Br−** (DET); Red: outer-sphere electron transfer from MiB• to **11•+Br−** to form **11-Br−** (OSET-I); Blue: outer-sphere electron transfer from MiB• to **11•+** (OSET-II); Magenta: associative electron transfer involving a termolecular encounter (AET-ter). Activation free energies in the OSET pathways were calculated using the Marcus theory.

Comparison between deactivation rates of the different pathways for Ph-PTZ

Rate of radical termination

The rate of radical termination was estimated from

$$R_t = k_t[R^\bullet]^2 = \left(10^7\ M^{-1}\ s^{-1}\right)\left(4.62\times10^{-8}\ M\right)^2 = 2.1\times10^{-8}\ M\ s^{-1}$$

$[R^\bullet]$ was calculated from $k_p^{app} = k_p[R^\bullet]$, using $k_p = 10^3\ M^{-1}s^{-1}$ and a value of k_p^{app} of $4.62\times10^{-5}\ s^{-1}$, estimated for photoinduced ATRP, with **2** as catalyst and MBiB as initiator, under 4.9 mW/cm^2 irradiation (Fig. 2 in the main text). We then compared this termination rate to the deactivation rate, considering that, in a controlled process, deactivation must be faster than radical termination.

Rate of termolecular AET deactivation pathway (AET-ter)

As already seen, the exact reverse process of metal-free ATRP activation is the termolecular AET deactivation reaction.

$$\mathbf{2}^{\bullet+} + X^- + R^\bullet \xrightarrow{k_{AET\text{-}ter}} \mathbf{2} + RX$$

In the literature, the rate of termolecular reactions was often considered to be very slow because of the low likelihood of a three-center simultaneous encounter. Nevertheless, in rare cases the exact calculation was carried out.

The frequency factor Z_{ter} for a termolecular reaction can be calculated following Tolman's approach:[23]

$$Z_{\text{ter}} = N_{\text{A}}^2 8\pi^2 \left(\frac{2RT}{\pi}\right)^{1/2} \left[\left(\frac{m_{\text{A}} + m_{\text{B}}}{m_{\text{A}} m_{\text{B}}}\right)^{1/2} + \left(\frac{m_{\text{B}} + m_{\text{C}}}{m_{\text{B}} m_{\text{C}}}\right)^{1/2}\right] d_{\text{A}\leftrightarrow\text{B}}^2 d_{\text{B}\leftrightarrow\text{C}}^2 \delta = 2.6\times10^{10}\ \text{M}^{-2}\ \text{s}^{-1}$$

where A, B and C are the three species involved in the reaction. d is the center-to-center distance between the subscript particles. δ is the distance between the two first spheres when hit by the third. Usually δ is taken to be between 0.3 Å[24] and 1 Å.[25] The smaller value, 0.3 Å, was used.

If we define A = **2**, B = Br^- and C =$R^\bullet$, then m_A = 0.27537 kg mol^{-1}, m_B = 0.0799 kg mol^{-1}, m_C = 0.101 kg mol^{-1}. r_A = 4.08 Å; r_B = 1.96 Å;[15] and r_C = 2.95 Å. With these values, Z_{ter} = 2.6×10^{10} $M^{-2}s^{-1}$ was obtained. Using $\Delta G^{\ddagger}_{\text{AET-ter}} = 3.9\,\text{kcal}\,\text{mol}^{-1}$, the deactivation rate constant was then calculated as

$$k_{\text{AET-ter}} = Z_{\text{ter}} e^{\frac{-\Delta G^{\ddagger}_{\text{AET-ter}}}{RT}} = \left(2.6\times10^{10}\ \text{M}^{-2}\ \text{s}^{-1}\right) e^{\left(\frac{-3940\ \text{cal}\,\text{mol}^{-1}}{1.987\text{cal}\,\text{mol}^{-1}\text{K}^{-1}\times 298.15\ \text{K}}\right)} = 3.4\times10^{7}\ \text{M}^{-2}\ \text{s}^{-1}$$

The rate for the termolecular deactivation reaction is

$$R_{\text{AET-ter}} = k_{\text{AET-ter}}[2^{\bullet+}][\text{Br}^-][\text{R}^\bullet]$$

Therefore, estimates for both $[2^{\bullet+}]$ and $[Br^-]$ are needed. Considering around 10% of termination, $[Br^-]$ should be ca 5×10^{-3} M. Moreover, the CV registered during a metal-free ATRP showed an oxidation current compatible with the presence of around 5×10^{-3} M Br^-, generated after a few hours of polymerization (Figure S14).

$\mathbf{2}^{\bullet+}$ was not detected during the electrochemical measurements. Moreover, it is known that this cation slowly disappears by reaction with Br^-.[26] Therefore 5×10^{-4} M was chosen as a reasonable estimate of $[2^{\bullet+}]$.

On the basis of these estimates it is finally possible to calculate the termolecular deactivation rate as

$$R_{\text{AET-ter}} = k_{\text{AET-ter}}[2^{\bullet+}][\text{Br}^-][\text{R}^\bullet] = 3.9\times10^{-6}\ \text{M s}^{-1}$$

$k_{\text{AET-ter}}$ and $R_{\text{AET-ter}}$ were also calculated on the basis of the value of $\Delta G^{\ddagger}_{\text{AET-ter}}$ of 5.0 kcal mol^{-1} derived from the experimental data. Using the same values of Z, [$\mathbf{2}^{\bullet+}$], [R$^\bullet$] and [Br^-] used in the previous case gives

$$k_{\text{AET-ter}} = Z_{\text{ter}} e^{\frac{-\Delta G^{\ddagger}_{\text{AET-ter}}}{RT}} = \left(2.6\times10^{10}\ \text{M}^{-2}\ \text{s}^{-1}\right) e^{\left(\frac{-5000\ \text{cal mol}^{-1}}{1.987\text{cal mol}^{-1}\text{K}^{-1}\times298.15\ \text{K}}\right)} = 5.8\times10^{6}\ \text{M}^{-2}\ \text{s}^{-1}$$

$$R_{\text{AET-ter}} = k_{\text{AET-ter}}[2^{\bullet+}][\text{Br}^-][\text{R}^\bullet] = 6.8\times10^{-7}\ \text{M s}^{-1}$$

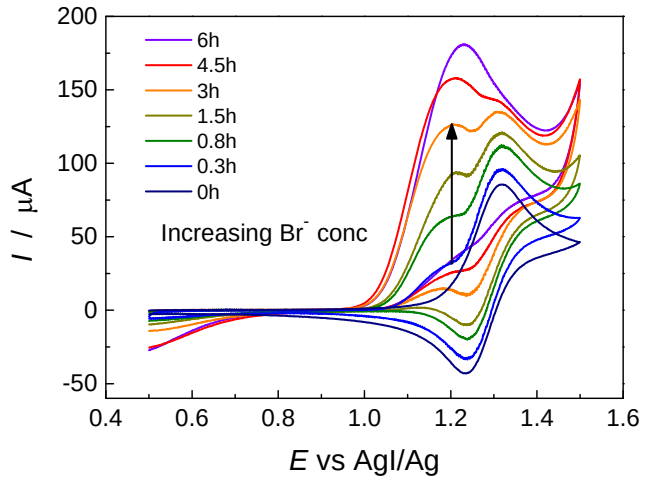

Figure S14. Cyclic voltammetry during photo-mediated experiment.

Rate of ISET deactivation pathway

The rate of the bimolecular deactivation reaction

$\mathbf{2}^{\bullet+}\mathrm{Br}^{-}\text{-C} + \mathrm{R}^{\bullet} \rightarrow \mathrm{RBr} + \mathbf{2}$

is given by

$$R_{\mathrm{ISET}} = k_{\mathrm{ISET}}[\mathbf{2}^{\bullet+}\mathrm{Br}^{-}\text{-C}][\mathrm{R}^{\bullet}]$$

where $\mathbf{2}^{\bullet+}\mathrm{Br}^{-}$-C is the ion pair adduct with covalent bond.

The deactivation rate constant, k_{ISET}, was calculated from the computed activation free energy ($\Delta G^{\neq}_{\mathrm{ISET}}$ = 10.5 kcal mol^{-1}) and the bimolecular collision frequency given by:

$$Z = N_{\mathrm{A}}\sqrt{\frac{8\pi RT}{\mu}}\left(r_{\mathbf{2}^{\bullet+}\mathbf{Br}^{-}} + r_{\mathrm{R}^{\bullet}}\right)$$

The reduced mass μ of the reagents $2^{\bullet+}Br^{-}$ and $MiB^{\bullet}$ is 0.07858 kg mol^{-1}, whereas their respective radii are 4.56×10^{-10} m and 2.95×10^{-10} m. Thus, Z = 3.02×10^{11} M^{-1}s^{-1}. Using this value together with $\Delta G^{\ddagger}_{\mathrm{ISET}} = 10.5\,\mathrm{kcal\,mol^{-1}}$ gives

$$k_{\mathrm{ISET}} = Ze^{\frac{-\Delta G^{\ddagger}_{\mathrm{ISET}}}{RT}} = \left(3.02\times10^{11}\ \mathrm{M^{-1}\,s^{-1}}\right)e^{\left(\frac{-10500\,\mathrm{cal\,mol^{-1}}}{1.987\mathrm{cal\,mol^{-1}K^{-1}}\times298.15\,\mathrm{K}}\right)} = 6.1\times10^{3}\ \mathrm{M^{-1}\,s^{-1}}$$

$\mathbf{2}^{\bullet+}\mathrm{Br}^{-}$-C must be formed by the association of $\mathbf{2}^{\bullet+}$ with Br^{-}. Therefore, its concentration can be obtained from the equilibrium constant of the reaction

$\mathbf{2}^{\bullet+} + \mathrm{Br}^{-} = \mathbf{2}^{\bullet+}\mathrm{Br}^{-}\text{-C}$

$\Delta_r G^{\ominus}$ of this reaction is 0.2 kcal mol^{-1}, which allowed the calculation of the formation equilibrium constant of $\mathbf{2}^{\bullet+}\mathbf{Br}^{-}$-**C**:

$$K_{\mathrm{f},\mathbf{2}^{\bullet+}\mathbf{Br}^{-}\text{-}\mathbf{C}} = e^{\frac{-\Delta G^{\ominus}}{RT}} = e^{\left(\frac{-200\,\mathrm{cal\,mol^{-1}}}{1.987\mathrm{cal\,mol^{-1}K^{-1}}\times 298.15\,\mathrm{K}}\right)} = 0.71$$

As in the case of the AET termolecular deactivation [$\mathbf{2}^{\bullet+}$] = 5×10^{-4} M and [Br^{-}] = 5×10^{-3} M can be used. Inserting these concentration values into the expression

$$K_{\mathrm{f},\mathbf{2}^{\bullet+}\mathbf{Br}^{-}} = \frac{[\mathbf{2}^{\bullet+}\mathbf{Br}^{-}\text{-C}]}{[\mathbf{2}^{\bullet+}][\mathrm{Br}^{-}]}$$

provides a very low equilibrium concentration of 1.8×10^{-6} M for $\mathbf{2}^{\bullet+}\mathbf{Br}^{-}$-**C**.

Therefore, the rate of deactivation was estimated as

$$R_{\mathrm{ISET}} = k_{\mathrm{ISET}}[\mathbf{2}^{\bullet+}\mathbf{Br}^{-}\text{-}\mathbf{C}][\mathrm{R}^{\bullet}] = 5.0\times10^{-10}\ \mathrm{M\,s^{-1}}$$

This is unreasonably low as a deactivation rate, being more than two orders of magnitude lower than the rate of radical-radical termination.

Rate of OSET-II deactivation pathway

This reaction pathway involves two consecutive reactions

$$\mathbf{2}^{\bullet+} + \mathrm{R}^{\bullet} \underset{k_{\mathrm{b,OSET\text{-}II}}}{\overset{k_{\mathrm{OSET\text{-}II}}}{\rightleftharpoons}} \mathrm{R}^{+} + \mathbf{2}$$

$$\mathrm{R}^{+} + \mathrm{Br}^{-} \rightarrow \mathrm{RBr}$$

From the activation free energy of 9.16 kcal mol^{-1}, it is possible to calculate the rate constant for the bimolecular deactivation reaction, $k_{\text{OSET-II}}$. The collision frequency Z was calculated using a reduced mass μ of 0.07387 kg mol^{-1} for $\mathbf{2}^{\bullet+}$ and MiB$^{\bullet}$ and $r_{\mathbf{2}^{\bullet+}}$ = 4.08×10^{-10} m and $r_{\text{R}^{\bullet}}$ = 2.95×10^{-10} m.

$$Z = N_{\text{A}}\sqrt{\frac{8\pi RT}{\mu}}\left(r_{\mathbf{2}^{\bullet+}} + r_{\text{R}^{\bullet}}\right) = 2.73\times10^{11}\ \text{M}^{-1}\text{s}^{-1}$$

The rate constant is

$$k_{\text{OSET-II}} = Ze^{\frac{-\Delta G^{\ddagger}_{\text{OSET-II}}}{RT}} = \left(2.73.10^{11}\ \text{M}^{-1}\ \text{s}^{-1}\right)e^{\left(\frac{-9160\ \text{cal mol}^{-1}}{1.987\text{cal mol}^{-1}\text{K}^{-1}\times298.15\ \text{K}}\right)} = 5.3\times10^{4}\ \text{M}^{-1}\ \text{s}^{-1}$$

To calculate the overall rate of the OSET reaction, also the reverse reaction, *i. e.* the back electron transfer between R^{+} and **2** in the solvent cage, which is likely to be very fast, must be considered. The rate constant of the back electron transfer, $k_{\text{b,OSET-II}}$, was calculated from $k_{\text{OSET-II}}$ and the equilibrium constant of the reaction, $K_{\text{OSET-II}}$, derived from the reaction Gibbs free energy:

$$K_{\text{OSET-II}} = \frac{k_{\text{OSET-II}}}{k_{\text{b,OSET-II}}} = e^{\frac{-\Delta_{\text{r}}G^{\ominus}}{RT}} = e^{\left(\frac{-8600\ \text{cal mol}^{-1}}{1.987\text{cal mol}^{-1}\text{K}^{-1}\times298.15\ \text{K}}\right)} = 4.96\times10^{-7}$$

It follows that

$$k_{\text{b,OSET-II}} = \frac{k_{\text{OSET-II}}}{K_{\text{OSET-II}}} = \frac{5.26\times10^{4}\ \text{M}^{-1}\text{s}^{-1}}{4.96\times10^{-7}} = 1.06\times10^{11}\ \text{M}^{-1}\text{s}^{-1}$$

which confirms that the reaction between R^{+} and **2** is extremely fast.

The carbocation R^+ is also expected to react at a diffusion-controlled rate with Br^- to generate RBr:

$$R^+ + Br^- \xrightarrow{k_{diff}} RBr$$

k_{diff} for a bimolecular reaction can be estimated from the viscosity η of the solvent (for DMA, $\eta = 9.27\times10^{-4}$ Pa s):[27]

$$k_{diff} = \frac{8RT}{3\eta} = 7.13\times10^{9}\ M^{-1}s^{-1}$$

The reaction of R^+ with Br^- is about 15 times slower than the back electron transfer between **2** and R^+. Therefore, the steady-state approximation can be applied to the intermediate R^+, which is consumed by fast reactions with both **2** and Br^-:

$$\frac{d[R^+]}{dt} = k_{OSET-II}[\mathbf{2}^{\bullet+}][R^\bullet] - k_{b,OSET-II}[R^+][\mathbf{2}] - k_{diff}[R^+][Br^-] = 0$$

$$[R^+] = \frac{k_{OSET-II}[\mathbf{2}^{\bullet+}][R^\bullet]}{k_{b,OSET-II}[\mathbf{2}] + k_{diff}[Br^-]}$$

It is now possible to calculate the overall rate of OSET-II deactivation pathway. The reaction rate can be conveniently defined as the rate of formation of RBr:

$$R_{OSET-II} = \frac{d[RBr]}{dt} = k_{diff}[R^+][Br^-] = k_{diff}[Br^-]\frac{k_{OSET-II}[\mathbf{2}^{\bullet+}][R^\bullet]}{k_{b,OSET-II}[\mathbf{2}] + k_{diff}[Br^-]}$$

Using $[\mathbf{2}^{\bullet+}] = 5\times10^{-4}$ M, $[R^\bullet] = 4.62\times10^{-8}$ M and $[Br^-] = 5\times10^{-3}$ M, together with previously estimated values of k_{OSET}, $k_{b,OSET}$ and k_{diff} gives $R_{OSET-II} = 7.6\times10^{-8}$ M s^{-1}.

Rate of OSET-I deactivation pathway

Deactivation through OSET-I occurs according to the following sequence of reactions:

$\mathbf{2}^{\bullet+}\mathrm{Br}^- + \mathrm{R}^\bullet \rightleftarrows \mathbf{2}\text{-}\mathrm{Br}^- + \mathrm{R}^+$

$\mathbf{2}\text{-}\mathrm{Br}^- \rightarrow \mathbf{2} + \mathrm{Br}^-$

$\mathrm{R}^+ + \mathrm{Br}^- \rightarrow \mathrm{RBr}$

Both decomposition of **2-Br**$^-$ and combination of R^+ with Br^- are much faster than electron transfer from $\mathbf{2}^{\bullet+}\mathbf{Br}^-$ to R, which is considered to the rate-determining step of the whole sequence. The overall rate of the deactivation pathway is assumed to be equal to the rate of the electron transfer and is calculated follows:

$$Z = N_\mathrm{A}\sqrt{\frac{8\pi RT}{\mu}}\left(r_{\mathbf{2}^{\bullet+}\mathbf{Br}^-} + r_{\mathrm{R}^\bullet}\right) = 3.02\times10^{11}\ \mathrm{M^{-1}s^{-1}}$$

for μ = 0.07872 kg mol^{-1}, $r_{\mathbf{2}^{\bullet+}\mathbf{Br}^-\text{-}\mathbf{C}} = 4.56\times10^{-10}$ m and $r_{\mathrm{R}^\bullet} = 2.95\times10^{-10}$ m.

$$k_\mathrm{OSET\text{-}I} = Ze^{\frac{-\Delta G^\ddagger_\mathrm{OSET\text{-}I}}{RT}} = \left(3.02\times10^{11}\ \mathrm{M^{-1}\ s^{-1}}\right)e^{\left(\frac{-13600\ \mathrm{cal\ mol^{-1}}}{1.987\mathrm{cal\ mol^{-1}K^{-1}}\times298.15\ \mathrm{K}}\right)} = 32.4\ \mathrm{M^{-1}\ s^{-1}}$$

$$R_\mathrm{OSET-I} = k_\mathrm{OSET\text{-}I}[\mathbf{2}^{\bullet+}\mathbf{Br}^-\text{-}\mathbf{C}][\mathrm{R}^\bullet] = 2.69\times10^{-12}\ \mathrm{M\ s^{-1}}$$

with $[\mathrm{R}^\bullet] = 4.62\times10^{-8}$ M and $[\mathbf{2}^{\bullet+}\mathbf{Br}^-\text{-}\mathrm{C}] = K_{\mathrm{f},\mathbf{2}^{\bullet+}\mathbf{Br}^-}[\mathbf{2}^{\bullet+}][\mathrm{Br}^-] = 1.8\times10^{-6}$ M .

Rate of DET deactivation pathway

The rate of the deactivation through dissociative electron transfer was calculated as previously described after estimating Z and $\Delta G^\ddagger$. The relevant reactions are

$\mathbf{2}^{\bullet+}\mathbf{Br}^-\text{-}\mathbf{C} + \mathrm{R}^\bullet \rightarrow \mathbf{2} + \mathrm{Br}^- + \mathrm{R}^+$

$R^+ + Br^- \rightarrow RBr$

and the rate-determining step is the DET reaction. As in the case of OSET-I, $\mu = 0.07872$ kg mol^{-1}, $r_{\mathbf{2}^{\bullet+}\mathbf{Br}^-\text{-}\mathbf{C}} = 4.56\times10^{-10}$ m and $r_{R^\bullet} = 2.95\times10^{-10}$ m, therefore $Z = 3.02\times10^{11}$ M^{-1}s^{-1}. The rate constant and the deactivation rate are

$$k_{DET} = Ze^{\frac{-\Delta G^{\ddagger}_{DET}}{RT}} = \left(3.02\times10^{11}\ M^{-1}\ s^{-1}\right)e^{\left(\frac{-14130\ cal\ mol^{-1}}{1.987 cal\ mol^{-1}K^{-1}\times298.15\ K}\right)} = 13.2\ M^{-1}\ s^{-1}$$

$$R_{DET} = k_{DET}[\mathbf{2}^{\bullet+}\mathbf{Br}^-\text{-}\mathbf{C}][R^\bullet] = 1.10\times10^{-12}\ M^{-1}\ s^{-1}$$

$\mathbf{11}^{\bullet+}$ deactivation vs. decomposition

Compared to **$\mathbf{2}^{\bullet+}$**, **$\mathbf{11}^{\bullet+}$** has very low barriers for deactivation (0.8 kcal mol^{-1} for both OSET-II and AET-ter pathways, as shown in Table 6 in the main text, and calculated applying the same model used for the catalyst **2**). Therefore, both OSET-II and AET-ter reactions are expected to proceed with diffusion rate constant, the bimolecular OSET-II being much faster because of the higher likelihood of bimolecular versus termolecular encounters.

Nevertheless, despite being potentially a very good deactivator, **$\mathbf{11}^{\bullet+}$** is too unstable (its lifetime is too slow) to provide any kind of deactivation. From the irreversible oxidation CV at $\upsilon = 100$ V s^{-1}, the lifetime of **$\mathbf{11}^{\bullet+}$** can be roughly estimated to be below 10^{-3} s. Therefore, assuming a first-order decomposition, the rate constant is $k_{decomp} > 10^3$ s^{-1}.

A comparison between rates of deactivation and decomposition shows that **$\mathbf{11}^{\bullet+}$** mainly undergoes decomposition rather than deactivation of $R^\bullet$.

$$\frac{R_{\text{decomp}}}{R_{\text{OSET-II}}} = \frac{k_{\text{decomp}}[\mathbf{11}^{\bullet+}]}{k_{\text{OSET-II}}[\mathbf{11}^{\bullet+}][\text{R}^{\bullet}]} > \frac{10^{3}\ \text{s}^{-1}}{\left(7\times10^{9}\ \text{M}^{-1}\ \text{s}^{-1}\right)\times\left(4.62\times10^{-8}\ \text{M}\right)} > 3.1$$

Since decomposition is faster than deactivation, the catalyst is quickly destroyed and, being unable to provide effective deactivation, the catalyst is lost after few activation/deactivation cycles.

Cartesian coordinates for optimized structures

Br-

B3LYP SCF energy:	-2571.84882301 a.u.
B3LYP enthalpy:	-2571.846463 a.u.
B3LYP free energy:	-2571.864999 a.u.
M06-2X SCF energy in solution:	-2574.34287547 a.u.
M06-2X enthalpy in solution:	-2574.340515 a.u.
M06-2X free energy in solution:	-2574.359051 a.u.

Cartesian coordinates

ATOM	X	Y	Z
Br	0.000000	0.000000	0.000000

Br$^{\bullet}$

B3LYP SCF energy:	-2571.66059539 a.u.
B3LYP enthalpy:	-2571.658235 a.u.
B3LYP free energy:	-2571.677425 a.u.
M06-2X SCF energy in solution:	-2574.13349445 a.u.
M06-2X enthalpy in solution:	-2574.131134 a.u.
M06-2X free energy in solution:	-2574.150324 a.u.

Cartesian coordinates

ATOM	X	Y	Z
Br	0.000000	0.000000	0.000000

Cl-

B3LYP SCF energy:	-460.36091178 a.u.
B3LYP enthalpy:	-460.358551 a.u.
B3LYP free energy:	-460.375935 a.u.
M06-2X SCF energy in solution:	-460.37364587 a.u.
M06-2X enthalpy in solution:	-460.371285 a.u.
M06-2X free energy in solution:	-460.388669 a.u.

Cartesian coordinates

ATOM	X	Y	Z
Cl	0.000000	0.000000	0.000000

Cl•

B3LYP SCF energy:	-460.13853491 a.u.
B3LYP enthalpy:	-460.136174 a.u.
B3LYP free energy:	-460.154212 a.u.
M06-2X SCF energy in solution:	-460.13619506 a.u.
M06-2X enthalpy in solution:	-460.133834 a.u.
M06-2X free energy in solution:	-460.151872 a.u.

Cartesian coordinates

ATOM	X	Y	Z
Cl	0.000000	0.000000	0.000000

MiB•

B3LYP SCF energy:	-346.37674180 a.u.
B3LYP enthalpy:	-346.233701 a.u.
B3LYP free energy:	-346.278420 a.u.
M06-2X SCF energy in solution:	-346.34347459 a.u.
M06-2X enthalpy in solution:	-346.200434 a.u.
M06-2X free energy in solution:	-346.245153 a.u.

Cartesian coordinates

ATOM	X	Y	Z
C	-1.090901	0.118125	0.019415
C	-2.199337	-0.878626	-0.020332
H	-1.822703	-1.899595	-0.110281
H	-2.816448	-0.811604	0.888910
H	-2.876638	-0.671792	-0.862521
C	-1.419362	1.575566	0.013092
H	-2.388743	1.758306	0.491526
H	-0.655274	2.176580	0.513256
H	-1.500817	1.953783	-1.019667
C	0.281321	-0.360864	0.009311
O	1.193152	0.650032	-0.009688
C	2.568829	0.242809	-0.009796
H	2.793739	-0.380676	-0.880294
H	3.149266	1.166211	-0.051127
H	2.814246	-0.312101	0.901142
O	0.614357	-1.545178	0.017053

MiB$^+$

B3LYP SCF energy:	-346.18707178 a.u.
B3LYP enthalpy:	-346.044151 a.u.
B3LYP free energy:	-346.087669 a.u.
M06-2X SCF energy in solution:	-346.14475548 a.u.
M06-2X enthalpy in solution:	-346.001835 a.u.
M06-2X free energy in solution:	-346.045353 a.u.

Cartesian coordinates

ATOM	X	Y	Z
C	-1.123795	0.048154	-0.048928
C	-1.903166	-1.037344	-0.618895
H	-1.434485	-2.018470	-0.514539
H	-2.948586	-1.017131	-0.300704
H	-1.900517	-0.805613	-1.708195
C	-1.694731	1.338997	0.299321
H	-2.773145	1.302729	0.462587
H	-1.154912	1.849125	1.104401
H	-1.506277	1.955606	-0.608005
C	0.329623	-0.179619	0.231369
O	1.176383	0.344990	-0.614108
C	2.600696	0.165396	-0.320562
H	2.840745	-0.898942	-0.310269
H	3.116016	0.672481	-1.133845
H	2.835409	0.628212	0.639215
O	0.532865	-0.805178	1.253549

MBiB

B3LYP SCF energy:	-2918.12916429 a.u.
B3LYP enthalpy:	-2917.981184 a.u.
B3LYP free energy:	-2918.027887 a.u.
M06-2X SCF energy in solution:	-2920.57010760 a.u.
M06-2X enthalpy in solution:	-2920.422127 a.u.
M06-2X free energy in solution:	-2920.468830 a.u.

Cartesian coordinates

ATOM	X	Y	Z
C	-0.089704	0.633200	-0.000008
C	-0.087677	1.484256	-1.271594
H	-0.104964	0.863889	-2.172799
H	-0.960208	2.143600	-1.285092
H	0.814727	2.104574	-1.294781
C	-0.087696	1.484321	1.271536
H	-0.960223	2.143671	1.284983
H	-0.105007	0.863999	2.172772
H	0.814713	2.104632	1.294712
C	1.089851	-0.357896	0.000031
O	2.240798	0.338868	0.000014
C	3.454645	-0.443617	0.000017
H	3.506333	-1.069980	-0.894088
H	4.266968	0.283762	0.000006
H	3.506339	-1.069953	0.894139
O	1.033095	-1.566547	-0.000025
Br	-1.789895	-0.438524	0.000010

MCiB

B3LYP SCF energy:	-806.61892169 a.u.
B3LYP enthalpy:	-806.470701 a.u.
B3LYP free energy:	-806.516431 a.u.
M06-2X SCF energy in solution:	-806.60012690 a.u.
M06-2X enthalpy in solution:	-806.451906 a.u.
M06-2X free energy in solution:	-806.497636 a.u.

Cartesian coordinates

ATOM	X	Y	Z
C	-0.648771	0.404455	0.000003
C	-0.776217	1.249086	-1.270910
H	-0.691841	0.632563	-2.171053
H	-1.741050	1.764112	-1.283590
H	0.018781	2.001040	-1.287099
C	-0.776250	1.249092	1.270908
H	-1.741088	1.764109	1.283565
H	-0.691886	0.632577	2.171057
H	0.018741	2.001054	1.287107
C	0.680196	-0.379457	0.000023
O	1.702688	0.492877	0.000003
C	3.026315	-0.086462	-0.000007
H	3.175463	-0.697179	-0.893845
H	3.714026	0.759505	-0.000042
H	3.175497	-0.697131	0.893859
O	0.814538	-1.581956	0.000014
Cl	-2.023888	-0.827547	-0.000011

[**MBiB**]$^{\bullet-}$

B3LYP SCF energy:	-2918.23430796 a.u.
B3LYP enthalpy:	-2918.088228 a.u.
B3LYP free energy:	-2918.139656 a.u.
M06-2X SCF energy in solution:	-2920.68856984 a.u.
M06-2X enthalpy in solution:	-2920.542490 a.u.
M06-2X free energy in solution:	-2920.593918 a.u.

Cartesian coordinates

ATOM	X	Y	Z
C	0.987009	0.373970	0.592659
C	0.183119	1.628493	0.563116
H	0.646257	2.396230	-0.061356
H	-0.834986	1.397218	0.202416
H	0.059586	2.038723	1.579279
C	0.396806	-0.808698	1.284492
H	-0.631634	-0.963274	0.913139
H	0.985076	-1.718548	1.151279
H	0.303145	-0.618415	2.366690
C	2.283280	0.350530	-0.056853
O	2.908106	-0.860613	0.030932
C	4.195653	-0.934739	-0.592145
H	4.893235	-0.219732	-0.144564
H	4.548488	-1.954039	-0.423925
H	4.125916	-0.737285	-1.666629
O	2.803180	1.306770	-0.634634
Br	-3.087445	-0.195642	-0.280981

[MCiB]$^{\bullet-}$

B3LYP SCF energy: -806.73903196 a.u.

B3LYP enthalpy: -806.592850 a.u.

B3LYP free energy: -806.645377 a.u.

M06-2X SCF energy in solution: -806.71806101 a.u.

M06-2X enthalpy in solution: -806.571879 a.u.

M06-2X free energy in solution: -806.624406 a.u.

Cartesian coordinates

ATOM	X	Y	Z
C	-0.337307	0.131960	-0.575596
C	0.560310	1.303927	-0.787171
H	0.105247	2.231002	-0.432565
H	1.522004	1.156075	-0.272247
H	0.804993	1.417456	-1.854756
C	0.126091	-1.214101	-1.026617
H	1.161391	-1.390290	-0.703859
H	-0.503707	-2.024236	-0.655208
H	0.136685	-1.270597	-2.127380
C	-1.642700	0.353115	0.024116
O	-2.385838	-0.783971	0.123035
C	-3.684173	-0.624448	0.711099
H	-4.311619	0.033522	0.101497
H	-4.117789	-1.625443	0.745397
H	-3.610601	-0.214049	1.722681
O	-2.061420	1.443225	0.412522
Cl	4.368125	-0.193541	0.536294

2

B3LYP SCF energy:	-1146.70155138 a.u.
B3LYP enthalpy:	-1146.426636 a.u.
B3LYP free energy:	-1146.486034 a.u.
M06-2X SCF energy in solution:	-1146.63452254 a.u.
M06-2X enthalpy in solution:	-1146.359607 a.u.
M06-2X free energy in solution:	-1146.419005 a.u.

Cartesian coordinates

ATOM	X	Y	Z
C	1.783052	3.683572	-0.493860
C	2.469441	2.558317	-0.034865
C	1.793048	1.356817	0.185596
C	0.417521	1.235846	-0.099158
C	-0.256827	2.374884	-0.570903
C	0.416320	3.584361	-0.750820
H	2.311802	4.620294	-0.643815
H	3.533678	2.614735	0.178284
H	-1.315747	2.321486	-0.792380
H	-0.139147	4.447768	-1.106807
C	1.793393	-1.356413	0.185618
C	2.470095	-2.557753	-0.034775
C	1.783993	-3.683217	-0.493688
C	0.417233	-3.584373	-0.750632
C	-0.256224	-2.375058	-0.570787
C	0.417831	-1.235808	-0.099138
H	3.534348	-2.613880	0.178372

H	2.312977	-4.619816	-0.643583
H	-0.138026	-4.447947	-1.106537
H	-1.315167	-2.321966	-0.792224
S	2.660175	0.000316	0.952481
N	-0.251699	-0.000070	0.100060
C	-1.693549	-0.000209	0.152776
C	-2.315952	0.000024	1.404631
C	-2.467116	-0.000525	-1.014582
C	-3.710035	-0.000064	1.489917
H	-1.703793	0.000260	2.302092
C	-3.860579	-0.000620	-0.924595
H	-1.976956	-0.000677	-1.983826
C	-4.483245	-0.000386	0.326567
H	-4.189684	0.000120	2.464895
H	-4.457779	-0.000865	-1.832348
H	-5.567807	-0.000453	0.393946

2*

B3LYP SCF energy:	-1146.60147443 a.u.
B3LYP enthalpy:	-1146.329744 a.u.
B3LYP free energy:	-1146.391040 a.u.
M06-2X SCF energy in solution:	-1146.52749649 a.u.
M06-2X enthalpy in solution:	-1146.255766 a.u.
M06-2X free energy in solution:	-1146.317062 a.u.

Cartesian coordinates

ATOM	X	Y	Z
C	-1.771855	-3.725374	-0.210224
C	-2.494725	-2.575634	-0.355201
C	-1.874378	-1.288637	-0.216378
C	-0.414602	-1.241227	0.013604
C	0.278075	-2.448386	0.233459
C	-0.363867	-3.671965	0.134997
H	-2.249454	-4.690687	-0.358441
H	-3.559615	-2.616141	-0.578089
H	1.342274	-2.425656	0.441524
H	0.187617	-4.590787	0.305110
C	-1.805871	1.391949	0.089924
C	-2.377681	2.677362	0.101123
C	-1.608114	3.806308	-0.118524
C	-0.223947	3.658374	-0.355760
C	0.362655	2.409072	-0.356195
C	-0.399163	1.231349	-0.118518
H	-3.448029	2.769954	0.267888
H	-2.068983	4.789215	-0.126103
H	0.392562	4.532542	-0.544691
H	1.425650	2.324000	-0.543409
S	-2.863058	0.032200	0.385624
N	0.235207	-0.010785	-0.051616
C	1.684098	-0.023720	0.000855
C	2.329522	0.235042	1.211371
C	2.411026	-0.305585	-1.157221

C	3.725028	0.212393	1.259425
H	1.743719	0.449375	2.100329
C	3.806066	-0.322108	-1.100895
H	1.886564	-0.504464	-2.087083
C	4.462892	-0.064586	0.105654
H	4.233333	0.409679	2.199082
H	4.377316	-0.534941	-2.000112
H	5.548565	-0.079553	0.146335

2$^{\bullet+}$

B3LYP SCF energy:	-1146.53293104 a.u.
B3LYP enthalpy:	-1146.257192 a.u.
B3LYP free energy:	-1146.316690 a.u.
M06-2X SCF energy in solution:	-1146.44927848 a.u.
M06-2X enthalpy in solution:	-1146.173539 a.u.
M06-2X free energy in solution:	-1146.233037 a.u.

Cartesian coordinates

ATOM	X	Y	Z
C	-1.663473	-3.778036	0.000002
C	-2.438161	-2.632567	0.000081
C	-1.832662	-1.364336	0.000013
C	-0.415800	-1.238834	-0.000123
C	0.350955	-2.429864	-0.000236
C	-0.261936	-3.667724	-0.000188

H	-2.138493	-4.753563	0.000082
H	-3.521831	-2.705005	0.000177
H	1.430433	-2.372044	-0.000441
H	0.353147	-4.561890	-0.000283
C	-1.833199	1.363696	0.000058
C	-2.439232	2.631669	0.000118
C	-1.665026	3.777464	-0.000052
C	-0.263453	3.667739	-0.000301
C	0.349956	2.430128	-0.000331
C	-0.416287	1.238773	-0.000164
H	-3.522931	2.703666	0.000330
H	-2.140464	4.752787	0.000032
H	0.351264	4.562158	-0.000463
H	1.429452	2.372803	-0.000518
S	-2.918467	-0.000536	0.000202
N	0.225668	0.000068	-0.000111
C	1.683755	0.000279	-0.000010
C	2.362690	0.000483	1.218583
C	2.362934	0.000251	-1.218477
C	3.758602	0.000718	1.211426
H	1.806832	0.000493	2.151101
C	3.758840	0.000487	-1.211039
H	1.807257	0.000049	-2.151103
C	4.455188	0.000731	0.000267
H	4.298537	0.000911	2.153651
H	4.298962	0.000476	-2.153156
H	5.541475	0.000932	0.000381

2-Br $^{-}$

B3LYP SCF energy:	-3718.55620930 a.u.
B3LYP enthalpy:	-3718.279515 a.u.
B3LYP free energy:	-3718.344176 a.u.
M06-2X SCF energy in solution:	-3720.97892892 a.u.
M06-2X enthalpy in solution:	-3720.702235 a.u.
M06-2X free energy in solution:	-3720.766896 a.u.
Imaginary frequency:	-5.6781 cm-1

Cartesian coordinates

ATOM	X	Y	Z
C	-2.304771	1.966394	-3.227531
C	-2.528037	2.196306	-1.868950
C	-1.943098	1.372248	-0.905530
C	-1.160768	0.260214	-1.279559
C	-0.954535	0.036207	-2.651738
C	-1.507866	0.887762	-3.609187
H	-2.745404	2.624271	-3.970895
H	-3.139582	3.035636	-1.548372
H	-0.351403	-0.803562	-2.974808
H	-1.318136	0.691043	-4.660937
C	-2.066617	0.170288	1.523130
C	-2.760654	-0.070241	2.710660
C	-2.639008	-1.296562	3.366236
C	-1.831881	-2.286123	2.806378
C	-1.168705	-2.065906	1.598227

C	-1.272435	-0.833379	0.930698
H	-3.378199	0.717912	3.133489
H	-3.165692	-1.469274	4.300266
H	-1.720037	-3.247260	3.300966
H	-0.559965	-2.856350	1.176447
S	-2.088645	1.808680	0.817652
N	-0.600658	-0.590212	-0.293584
C	0.493337	-1.456613	-0.668566
C	0.262173	-2.694092	-1.283633
C	1.798056	-1.030408	-0.405814
C	1.342336	-3.506698	-1.634958
H	-0.756455	-3.014158	-1.484792
C	2.872194	-1.850684	-0.761028
H	1.992673	-0.066116	0.069456
C	2.649913	-3.085997	-1.373512
H	1.161305	-4.465924	-2.112744
H	3.883169	-1.509564	-0.552731
H	3.489511	-3.719742	-1.647572
Br	3.444381	1.971411	1.038656

2-Br-TS1

B3LYP SCF energy:	-4064.78419119 a.u.
B3LYP enthalpy:	-4064.361298 a.u.
B3LYP free energy:	-4064.451720 a.u.
M06-2X SCF energy in solution:	-4067.58949578 a.u.

M06-2X enthalpy in solution: -4067.166603 a.u.

M06-2X free energy in solution: -4067.257025 a.u.

Imaginary frequency: -43.7732 cm-1

Cartesian coordinates

ATOM	X	Y	Z
C	2.952331	-1.855997	-3.288724
C	2.805215	-2.345364	-1.998530
C	2.434029	-1.484505	-0.954930
C	2.215729	-0.107416	-1.187849
C	2.363950	0.365881	-2.506923
C	2.722411	-0.496051	-3.535224
H	3.239085	-2.523559	-4.095143
H	2.966917	-3.398770	-1.787660
H	2.202808	1.415374	-2.719511
H	2.832530	-0.099402	-4.540285
C	2.346184	-0.819787	1.665135
C	2.639808	-1.074538	3.013095
C	2.713920	-0.028373	3.921817
C	2.488370	1.280972	3.477377
C	2.207114	1.544390	2.143051
C	2.134959	0.498880	1.200928
H	2.799980	-2.098617	3.338671
H	2.941153	-0.227632	4.964343
H	2.541255	2.109566	4.177637
H	2.047522	2.566067	1.822059
S	2.093312	-2.197040	0.610076

N	1.860136	0.764852	-0.148641
C	1.170536	1.993593	-0.486404
C	1.873138	3.174167	-0.739978
C	-0.224454	1.955491	-0.553320
C	1.162986	4.333355	-1.062446
H	2.957843	3.182488	-0.685776
C	-0.925021	3.118674	-0.877313
H	-0.738491	1.018317	-0.352656
C	-0.232541	4.306095	-1.130717
H	1.702662	5.255275	-1.260483
H	-2.009023	3.083522	-0.928497
H	-0.779600	5.210852	-1.382130
Br	-0.930806	-1.856327	0.413698
C	-4.276887	-1.055413	-0.628816
C	-3.810739	-1.358690	-2.012667
H	-3.673459	-0.447928	-2.600203
H	-2.841689	-1.880074	-1.965102
H	-4.511660	-2.026065	-2.531143
C	-4.733732	-2.170545	0.255157
H	-3.868308	-2.609545	0.776260
H	-5.440691	-1.835268	1.019089
H	-5.196334	-2.970519	-0.334798
C	-4.157022	0.308411	-0.142699
O	-4.526174	0.442239	1.159419
C	-4.434509	1.766680	1.700719
H	-5.061758	2.465822	1.139287
H	-4.790633	1.691001	2.729683

H	-3.400283	2.124213	1.690526
O	-3.782605	1.265956	-0.821763

$2^{\bullet+}$-Br-C

B3LYP SCF energy:	-3718.40298911 a.u.
B3LYP enthalpy:	-3718.124726 a.u.
B3LYP free energy:	-3718.192355 a.u.
M06-2X SCF energy in solution:	-3720.79940149 a.u.
M06-2X enthalpy in solution:	-3720.521138 a.u.
M06-2X free energy in solution:	-3720.588767 a.u.

Cartesian coordinates

ATOM	X	Y	Z
C	-1.133918	3.724349	-1.437760
C	-1.914353	2.591452	-1.252828
C	-1.311498	1.357189	-0.968917
C	0.093643	1.235438	-0.878259
C	0.865498	2.399536	-1.062516
C	0.258929	3.619586	-1.333626
H	-1.602811	4.678505	-1.656802
H	-2.997074	2.653011	-1.316763
H	1.944867	2.341601	-0.999104
H	0.882478	4.497564	-1.475128
C	-1.316010	-1.346977	-0.974422
C	-1.923009	-2.578036	-1.263240

C	-1.146395	-3.712917	-1.452185
C	0.246755	-3.613345	-1.347198
C	0.857427	-2.396389	-1.071383
C	0.089505	-1.230373	-0.882972
H	-3.005918	-2.635661	-1.327679
H	-1.618503	-4.664642	-1.674871
H	0.867318	-4.492951	-1.491719
H	1.936964	-2.342377	-1.007379
S	-2.357937	0.006064	-0.572610
N	0.705753	0.000986	-0.611710
C	2.034629	-0.002303	-0.036501
C	3.175783	-0.002724	-0.842656
C	2.136653	-0.005011	1.357100
C	4.436209	-0.005862	-0.239864
H	3.075011	-0.000599	-1.924066
C	3.400470	-0.008111	1.949444
H	1.225179	-0.004752	1.950253
C	4.548943	-0.008539	1.152922
H	5.328077	-0.006210	-0.860155
H	3.486646	-0.010180	3.032553
H	5.531423	-0.010942	1.616911
Br	-1.790357	-0.005945	2.402482

$2^{\bullet+}$-Br-I

B3LYP SCF energy:	-3718.39835486 a.u.
B3LYP enthalpy:	-3718.119991 a.u.
B3LYP free energy:	-3718.187008 a.u.
M06-2X SCF energy in solution:	-3720.80089529 a.u.
M06-2X enthalpy in solution:	-3720.522531 a.u.
M06-2X free energy in solution:	-3720.589548 a.u.

Cartesian coordinates

ATOM	X	Y	Z
C	-0.471566	4.201497	0.074424
C	-1.439704	3.308295	-0.360420
C	-1.118882	1.963427	-0.594888
C	0.198030	1.487672	-0.386135
C	1.166584	2.417544	0.053196
C	0.836644	3.745570	0.277936
H	-0.731511	5.239732	0.255232
H	-2.459990	3.645773	-0.521322
H	2.183937	2.092794	0.223425
H	1.607648	4.429819	0.618921
C	-1.727625	-0.646460	-1.084967
C	-2.596333	-1.715810	-1.357552
C	-2.123044	-3.014899	-1.407282
C	-0.759037	-3.260821	-1.177933
C	0.109300	-2.224365	-0.895661
C	-0.342834	-0.880644	-0.842747
H	-3.647493	-1.508648	-1.537716

H	-2.802326	-3.833391	-1.623798
H	-0.375488	-4.275813	-1.216751
H	1.154051	-2.441577	-0.722275
S	-2.412707	0.954110	-1.216980
N	0.560835	0.150934	-0.618348
Br	-1.329372	-0.814561	2.247153
C	1.943254	-0.214282	-0.362344
C	2.871279	-0.160608	-1.401682
C	2.310488	-0.607649	0.926866
C	4.199646	-0.506740	-1.142387
H	2.555636	0.147649	-2.394034
C	3.640621	-0.951249	1.173015
H	1.548261	-0.654156	1.701738
C	4.583888	-0.899969	0.142030
H	4.931029	-0.469071	-1.944758
H	3.939407	-1.260427	2.170805
H	5.618077	-1.168421	0.339455

2-Cl $^-$

B3LYP SCF energy:	-1607.06387816 a.u.
B3LYP enthalpy:	-1606.786187 a.u.
B3LYP free energy:	-1606.854034 a.u.
M06-2X SCF energy in solution:	-1607.00903175 a.u.
M06-2X enthalpy in solution:	-1606.731341 a.u.
M06-2X free energy in solution:	-1606.799188 a.u.

Cartesian coordinates

ATOM	X	Y	Z
C	-2.291395	3.675488	0.857213
C	-3.087725	2.554311	0.618362
C	-2.512256	1.355744	0.191822
C	-1.115529	1.234073	0.043575
C	-0.326555	2.368301	0.299210
C	-0.911077	3.575177	0.686391
H	-2.747131	4.610412	1.169806
H	-4.166099	2.611460	0.740249
H	0.749635	2.311977	0.189484
H	-0.272409	4.435602	0.866555
C	-2.512215	-1.355746	0.191911
C	-3.087649	-2.554292	0.618549
C	-2.291287	-3.675438	0.857456
C	-0.910979	-3.575112	0.686567
C	-0.326492	-2.368249	0.299285
C	-1.115494	-1.234050	0.043626
H	-4.166021	-2.611456	0.740456
H	-2.746992	-4.610348	1.170135
H	-0.272285	-4.435517	0.866743
H	0.749691	-2.311909	0.189501
S	-3.568783	-0.000033	-0.285559
N	-0.543043	0.000009	-0.359937
C	0.800908	-0.000018	-0.886304
C	0.970692	-0.000213	-2.274156

C	1.919442	0.000115	-0.043546
C	2.256890	-0.000273	-2.818496
H	0.094582	-0.000310	-2.916479
C	3.205244	0.000054	-0.590046
H	1.779959	0.000260	1.033961
C	3.372764	-0.000138	-1.977946
H	2.384614	-0.000417	-3.897668
H	4.073691	0.000173	0.067479
H	4.373288	-0.000184	-2.402424
Cl	6.402563	0.000135	1.673522

$2^{\bullet+}$-Cl-C

B3LYP SCF energy:	-1606.89573696 a.u.
B3LYP enthalpy:	-1606.617245 a.u.
B3LYP free energy:	-1606.686294 a.u.
M06-2X SCF energy in solution:	-1606.82639208 a.u.
M06-2X enthalpy in solution:	-1606.547900 a.u.
M06-2X free energy in solution:	-1606.616949 a.u.

Cartesian coordinates

ATOM	X	Y	Z
C	1.142862	-3.776504	-0.683226
C	1.898893	-2.626646	-0.816252
C	1.307346	-1.359452	-0.659556
C	-0.075717	-1.238599	-0.360566

C	-0.824075	-2.431907	-0.228936
C	-0.225900	-3.669274	-0.386484
H	1.606797	-4.749772	-0.806295
H	2.959318	-2.691079	-1.042546
H	-1.879778	-2.379457	-0.000970
H	-0.830342	-4.564409	-0.277531
C	1.307268	1.359578	-0.659508
C	1.898739	2.626811	-0.816176
C	1.142642	3.776621	-0.683114
C	-0.226113	3.669303	-0.386368
C	-0.824213	2.431896	-0.228845
C	-0.075784	1.238635	-0.360503
H	2.959158	2.691312	-1.042482
H	1.606517	4.749919	-0.806166
H	-0.830608	4.564398	-0.277392
H	-1.879915	2.379377	-0.000887
S	2.382051	0.000097	-0.813013
N	-0.701744	-0.000002	-0.200405
Cl	4.022253	-0.000053	2.100116
C	-2.112990	-0.000049	0.149322
C	-2.476907	-0.000126	1.496260
C	-3.072303	-0.000010	-0.864214
C	-3.831871	-0.000166	1.831916
H	-1.709032	-0.000154	2.264126
C	-4.424497	-0.000052	-0.516762
H	-2.761255	0.000052	-1.904507
C	-4.803824	-0.000128	0.828089

H	-4.125005	-0.000226	2.877720
H	-5.178906	-0.000021	-1.298225
H	-5.857183	-0.000159	1.093759

$2^{\bullet+}$-Cl-I

B3LYP SCF energy:	-1606.89766749 a.u.
B3LYP enthalpy:	-1606.619179 a.u.
B3LYP free energy:	-1606.687645 a.u.
M06-2X SCF energy in solution:	-1606.82776560 a.u.
M06-2X enthalpy in solution:	-1606.549277 a.u.
M06-2X free energy in solution:	-1606.617743 a.u.

Cartesian coordinates

ATOM	X	Y	Z
C	-1.703608	3.777506	-0.389535
C	-2.477703	2.631876	-0.363972
C	-1.872708	1.363876	-0.392103
C	-0.457042	1.238313	-0.446740
C	0.308991	2.429627	-0.473591
C	-0.303226	3.667406	-0.445158
H	-2.178372	4.752920	-0.366331
H	-3.560538	2.704152	-0.320972
H	1.387585	2.371557	-0.514717
H	0.311547	4.561577	-0.465258
C	-1.872515	-1.363912	-0.392445

C	-2.477335	-2.632002	-0.364658
C	-1.703078	-3.777519	-0.390436
C	-0.302705	-3.667206	-0.445863
C	0.309341	-2.429332	-0.473953
C	-0.456866	-1.238136	-0.446976
H	-3.560163	-2.704435	-0.321736
H	-2.177708	-4.753004	-0.367516
H	0.312199	-4.561284	-0.466074
H	1.387933	-2.371106	-0.514886
S	-2.957370	-0.000100	-0.355662
N	0.183958	0.000140	-0.474487
C	1.642628	0.000236	-0.520338
C	2.281788	0.000266	-1.760516
C	2.354878	0.000280	0.679154
C	3.677248	0.000340	-1.796879
H	1.697220	0.000225	-2.675482
C	3.750497	0.000350	0.624532
H	1.823575	0.000258	1.631256
C	4.410233	0.000378	-0.607113
H	4.188207	0.000363	-2.755248
H	4.320041	0.000383	1.549594
H	5.496165	0.000431	-0.640652
Cl	0.348801	-0.000911	3.863504

2-Cl-TS1

B3LYP SCF energy: -1953.27154089 a.u.

B3LYP enthalpy: -1952.848851 a.u.

B3LYP free energy: -1952.938935 a.u.

M06-2X SCF energy in solution: -1953.17187948 a.u.

M06-2X enthalpy in solution: -1952.749190 a.u.

M06-2X free energy in solution: -1952.839274 a.u.

Imaginary frequency: -91.0729 cm-1

Cartesian coordinates

ATOM	X	Y	Z
C	2.518787	-2.884673	-2.716648
C	2.005826	-3.202639	-1.469786
C	1.735452	-2.193639	-0.530329
C	1.988924	-0.832463	-0.832292
C	2.505127	-0.534833	-2.112831
C	2.762019	-1.540487	-3.032128
H	2.725370	-3.669444	-3.437258
H	1.802166	-4.237138	-1.207504
H	2.709397	0.492549	-2.382586
H	3.160837	-1.272904	-4.006035
C	1.149663	-1.289717	1.966341
C	0.877342	-1.462753	3.333699
C	0.892597	-0.380111	4.197613
C	1.179985	0.894535	3.689633
C	1.456270	1.079535	2.343399
C	1.454164	-0.008761	1.442627

H	0.648161	-2.457519	3.705657
H	0.681227	-0.521580	5.252679
H	1.194037	1.754530	4.352424
H	1.683011	2.073763	1.982511
S	0.979212	-2.705601	0.958184
N	1.742615	0.195384	0.087063
C	1.859000	1.564571	-0.380483
C	3.094559	2.214346	-0.334262
C	0.720138	2.208112	-0.867517
C	3.188450	3.532602	-0.784087
H	3.965856	1.692445	0.050288
C	0.826114	3.527151	-1.314932
H	-0.234193	1.689472	-0.894141
C	2.055810	4.188813	-1.273849
H	4.145920	4.044542	-0.750472
H	-0.056161	4.034905	-1.694347
H	2.132273	5.214962	-1.622654
C	-4.273666	-0.173864	-1.006792
C	-4.142476	-0.529494	-2.448636
H	-3.220887	-0.133834	-2.880432
H	-4.175897	-1.615486	-2.591857
H	-4.987887	-0.111871	-3.021932
C	-5.360715	-0.799742	-0.197203
H	-5.157722	-0.756330	0.874710
H	-6.316495	-0.275524	-0.369977
H	-5.515279	-1.843388	-0.491766
C	-3.515606	0.969542	-0.510503

O	-3.831009	1.296101	0.769117
C	-3.110446	2.402970	1.327865
H	-3.232410	3.301678	0.716437
H	-3.537936	2.563229	2.319266
H	-2.044628	2.169857	1.416822
O	-2.697108	1.608246	-1.170800
Cl	-1.953731	-1.996692	0.059991

8

B3LYP SCF energy:	-954.96395849 a.u.
B3LYP enthalpy:	-954.744341 a.u.
B3LYP free energy:	-954.794262 a.u.
M06-2X SCF energy in solution:	-954.91260992 a.u.
M06-2X enthalpy in solution:	-954.692992 a.u.
M06-2X free energy in solution:	-954.742913 a.u.

Cartesian coordinates

ATOM	X	Y	Z
C	-3.642232	-0.670438	0.628233
C	-2.542649	-1.444076	0.248972
C	-1.351725	-0.830943	-0.141381
C	-1.218460	0.572896	-0.122809
C	-2.323433	1.336630	0.288956
C	-3.525233	0.718845	0.642873
H	-4.573568	-1.152373	0.911062

H	-2.612782	-2.528487	0.237804
H	-2.250559	2.417065	0.336170
H	-4.367252	1.335966	0.944598
C	1.351786	-0.830872	-0.141460
C	2.542730	-1.443990	0.248866
C	3.642296	-0.670344	0.628159
C	3.525222	0.718924	0.642948
C	2.323420	1.336702	0.289021
C	1.218491	0.572973	-0.122911
H	2.612882	-2.528399	0.237664
H	4.573639	-1.152265	0.910989
H	4.367191	1.336051	0.944809
H	2.250510	2.417119	0.336432
S	0.000046	-1.817157	-0.764526
N	-0.000026	1.170703	-0.520865
C	-0.000191	2.602661	-0.804122
H	-0.884027	2.847590	-1.397236
H	-0.000081	3.225746	0.101684
H	0.883351	2.847771	-1.397585

8*

B3LYP SCF energy:	-954.85941342 a.u.
B3LYP enthalpy:	-954.642824 a.u.
B3LYP free energy:	-954.695713 a.u.
M06-2X SCF energy in solution:	-954.80033614 a.u.

M06-2X enthalpy in solution: -954.583747 a.u.

M06-2X free energy in solution: -954.636636 a.u.

Cartesian coordinates

ATOM	X	Y	Z
C	-3.730947	-0.717151	0.364288
C	-2.584348	-1.456607	0.399832
C	-1.297532	-0.845650	0.204688
C	-1.243528	0.616799	-0.032482
C	-2.453849	1.331247	-0.095179
C	-3.680705	0.705073	0.091692
H	-4.689869	-1.191259	0.558946
H	-2.622796	-2.527518	0.590254
H	-2.444587	2.407242	-0.225971
H	-4.596790	1.285218	0.057802
C	1.363372	-0.832140	-0.131582
C	2.634845	-1.428014	-0.089777
C	3.769285	-0.676395	0.171207
C	3.635316	0.708093	0.405041
C	2.397298	1.318661	0.346004
C	1.218342	0.579880	0.048351
H	2.713622	-2.501471	-0.242504
H	4.742199	-1.155233	0.223870
H	4.508817	1.306181	0.648810
H	2.328184	2.377442	0.563359
S	-0.017063	-1.852291	-0.457603
N	-0.003630	1.235682	-0.118810

C	0.020284	2.675190	-0.426335
H	-0.737800	2.890649	-1.179129
H	-0.175871	3.275835	0.468245
H	0.986304	2.945871	-0.844852

8$^{\bullet+}$

B3LYP SCF energy:	-954.79331177 a.u.
B3LYP enthalpy:	-954.572776 a.u.
B3LYP free energy:	-954.623683 a.u.
M06-2X SCF energy in solution:	-954.72477091 a.u.
M06-2X enthalpy in solution:	-954.504235 a.u.
M06-2X free energy in solution:	-954.555142 a.u.

Cartesian coordinates

ATOM	X	Y	Z
C	-3.747787	-0.666186	0.260609
C	-2.616832	-1.440549	0.069322
C	-1.357158	-0.833490	-0.060886
C	-1.228137	0.582125	-0.022710
C	-2.399629	1.347457	0.193562
C	-3.629497	0.732535	0.334197
H	-4.717293	-1.141694	0.367711
H	-2.694107	-2.522991	0.027855
H	-2.336194	2.423351	0.284895
H	-4.508799	1.342853	0.513793

C	1.357132	-0.833494	-0.060719
C	2.616780	-1.440574	0.069626
C	3.747766	-0.666220	0.260758
C	3.629536	0.732526	0.333999
C	2.399696	1.347472	0.193255
C	1.228142	0.582140	-0.022766
H	2.694012	-2.523027	0.028348
H	4.717249	-1.141745	0.368000
H	4.508879	1.342849	0.513376
H	2.336332	2.423396	0.284274
S	0.000005	-1.896505	-0.333936
N	0.000006	1.216053	-0.194149
C	-0.000026	2.656409	-0.521043
H	0.000133	3.264218	0.388854
H	0.880252	2.881786	-1.119298
H	-0.880491	2.881813	-1.119012

8-Br$^-$

B3LYP SCF energy:	-3526.82125639 a.u.
B3LYP enthalpy:	-3526.598817 a.u.
B3LYP free energy:	-3526.657463 a.u.
M06-2X SCF energy in solution:	-3529.25793553 a.u.
M06-2X enthalpy in solution:	-3529.035496 a.u.
M06-2X free energy in solution:	-3529.094142 a.u.

Cartesian coordinates

ATOM	X	Y	Z
C	-0.282691	-3.626453	0.587133
C	1.021197	-3.175195	0.368714
C	1.244497	-1.876118	-0.089605
C	0.171353	-0.986957	-0.303020
C	-1.134691	-1.437412	-0.042161
C	-1.350058	-2.751848	0.380655
H	-0.455278	-4.644945	0.923754
H	1.867530	-3.835881	0.537593
H	-1.988147	-0.763781	-0.133342
H	-2.369064	-3.081706	0.568139
C	2.745627	0.375534	-0.012806
C	3.843986	1.059198	0.509306
C	3.761418	2.428961	0.772615
C	2.559351	3.096422	0.538371
C	1.445116	2.409067	0.051727
C	1.521517	1.037674	-0.246924
H	4.770531	0.520772	0.690683
H	4.625891	2.961035	1.159133
H	2.474084	4.159250	0.748846
H	0.511958	2.942537	-0.090152
S	2.900314	-1.338110	-0.493420
N	0.426526	0.322525	-0.772682
Br	-4.144255	0.897756	0.187774
C	-0.688672	1.068069	-1.358137
H	-1.430679	1.421201	-0.629483

H	-0.285496	1.914768	-1.919381
H	-1.210823	0.411701	-2.059612

$8^{\bullet+}$-Br-C

B3LYP SCF energy:	-3526.66288398 a.u.
B3LYP enthalpy:	-3526.439740 a.u.
B3LYP free energy:	-3526.498880 a.u.
M06-2X SCF energy in solution:	-3529.07637786 a.u.
M06-2X enthalpy in solution:	-3528.853234 a.u.
M06-2X free energy in solution:	-3528.912374 a.u.

Cartesian coordinates

ATOM	X	Y	Z
C	3.704774	-0.791481	-1.061520
C	2.580711	-0.082166	-1.463434
C	1.349247	-0.285941	-0.824336
C	1.222293	-1.211256	0.238142
C	2.372993	-1.932324	0.617392
C	3.590762	-1.717838	-0.018229
H	4.656461	-0.630544	-1.558203
H	2.646351	0.638019	-2.274298
H	2.311517	-2.677473	1.401013
H	4.457321	-2.291857	0.297077
C	-1.349553	-0.285300	-0.824302
C	-2.580944	-0.080951	-1.463361

C	-3.705329	-0.789729	-1.061399
C	-3.591728	-1.716114	-0.018087
C	-2.374041	-1.931167	0.617499
C	-1.223011	-1.210668	0.238179
H	-2.646278	0.639248	-2.274238
H	-4.656953	-0.628353	-1.558059
H	-4.458553	-2.289707	0.297263
H	-2.312892	-2.676310	1.401154
S	0.000081	0.728550	-1.308782
N	-0.000400	-1.411176	0.888484
Br	0.000936	2.843400	0.810359
C	-0.000571	-2.078623	2.193004
H	-0.000860	-3.171873	2.104822
H	0.881334	-1.763925	2.752386
H	-0.882325	-1.763467	2.752369

$8^{\bullet+}$-Br-I

B3LYP SCF energy:	-3526.65729029 a.u.
B3LYP enthalpy:	-3526.434205 a.u.
B3LYP free energy:	-3526.493236 a.u.
M06-2X SCF energy in solution:	-3529.07527117 a.u.
M06-2X enthalpy in solution:	-3528.852186 a.u.
M06-2X free energy in solution:	-3528.911217 a.u.

Cartesian coordinates

ATOM	X	Y	Z
C	-3.826492	0.310252	0.569698
C	-2.722205	0.343575	1.411737
C	-1.510418	-0.233336	1.012966
C	-1.392122	-0.867421	-0.247182
C	-2.521771	-0.876597	-1.092634
C	-3.716536	-0.297752	-0.687389
H	-4.762048	0.762479	0.883991
H	-2.788936	0.822064	2.384751
H	-2.457965	-1.315289	-2.080393
H	-4.566974	-0.312284	-1.362537
C	1.181269	-0.436616	1.088738
C	2.451077	-0.093391	1.575235
C	3.583959	-0.346964	0.818472
C	3.453268	-0.935605	-0.449679
C	2.208296	-1.280947	-0.945760
C	1.037180	-1.061065	-0.181650
H	2.536335	0.372455	2.552794
H	4.563981	-0.079928	1.201744
H	4.334378	-1.114908	-1.058596
H	2.133557	-1.706465	-1.938023
S	-0.186399	-0.253287	2.172522
N	-0.201823	-1.490815	-0.639947
Br	0.523746	2.124612	-0.897059
C	-0.248717	-2.432436	-1.764178
H	-0.185421	-1.917872	-2.730076

H	0.576638	-3.138107	-1.674031
H	-1.180227	-2.995476	-1.713512

8-Br-TS1

B3LYP SCF energy:	-3873.04158241 a.u.
B3LYP enthalpy:	-3872.674159 a.u.
B3LYP free energy:	-3872.759606 a.u.
M06-2X SCF energy in solution:	-3875.42228525 a.u.
M06-2X enthalpy in solution:	-3875.054862 a.u.
M06-2X free energy in solution:	-3875.140309 a.u.
Imaginary frequency:	-30.3639 cm-1

Cartesian coordinates

ATOM	X	Y	Z
C	-2.878666	-3.762137	-0.522481
C	-2.463928	-2.673577	-1.278582
C	-2.312572	-1.413971	-0.681466
C	-2.577391	-1.221950	0.694685
C	-3.012586	-2.337446	1.438545
C	-3.151909	-3.584048	0.838843
H	-2.993353	-4.736099	-0.987805
H	-2.249669	-2.789865	-2.337418
H	-3.260911	-2.224422	2.486588
H	-3.491183	-4.422505	1.440253
C	-2.303116	1.281696	-0.807245

C	-2.447875	2.480736	-1.519724
C	-2.856604	3.637330	-0.868670
C	-3.130563	3.588589	0.503259
C	-2.998162	2.402806	1.217072
C	-2.569127	1.220285	0.580729
H	-2.234338	2.496078	-2.584919
H	-2.966605	4.564190	-1.422861
H	-3.465331	4.481433	1.023492
H	-3.246958	2.390571	2.271107
S	-1.669468	-0.111540	-1.668526
N	-2.418421	0.029489	1.299497
Br	1.200310	-0.093398	-0.817313
C	4.724011	-0.892006	0.114495
C	4.766545	-2.185560	0.854041
H	4.564458	-2.047161	1.918404
H	4.023690	-2.890078	0.447720
H	5.744634	-2.675069	0.736082
C	5.001583	-0.861247	-1.354509
H	4.066280	-0.697544	-1.910181
H	5.677847	-0.042762	-1.629327
H	5.439305	-1.805637	-1.694331
C	4.322561	0.309543	0.828193
O	4.334367	1.414202	0.033869
C	3.752728	2.589917	0.607148
H	4.260406	2.878048	1.532394
H	3.870915	3.375764	-0.141866
H	2.689464	2.423794	0.806011

O	4.017801	0.355057	2.018802
C	-2.325990	0.098452	2.760450
H	-1.768531	0.994263	3.037109
H	-3.310443	0.123816	3.243090
H	-1.771086	-0.768219	3.122273

11

B3LYP SCF energy:	-748.53842536 a.u.
B3LYP enthalpy:	-748.266153 a.u.
B3LYP free energy:	-748.322480 a.u.
M06-2X SCF energy in solution:	-748.46167519 a.u.
M06-2X enthalpy in solution:	-748.189403 a.u.
M06-2X free energy in solution:	-748.245730 a.u.

Cartesian coordinates

ATOM	X	Y	Z
C	2.595646	3.043594	-0.000125
C	2.952712	1.696950	0.000049
C	1.943278	0.724544	-0.000013
C	0.581858	1.131676	-0.000290
C	0.217129	2.481730	-0.000429
C	1.241197	3.427494	-0.000348
H	3.368947	3.806988	-0.000103
H	3.999409	1.403309	0.000239
H	-0.825710	2.783348	-0.000599

H	0.985338	4.483898	-0.000461
C	1.943274	-0.724551	0.000103
C	2.952704	-1.696963	0.000424
C	2.595631	-3.043603	0.000429
C	1.241179	-3.427497	0.000140
C	0.217117	-2.481729	-0.000181
C	0.581852	-1.131676	-0.000215
H	3.999402	-1.403325	0.000661
H	3.368926	-3.807004	0.000639
H	0.985317	-4.483900	0.000184
H	-0.825725	-2.783341	-0.000382
N	-0.231790	0.000002	-0.000463
C	-1.663736	0.000004	-0.000150
C	-2.358794	0.000804	1.213968
C	-2.359276	-0.000796	-1.213980
C	-3.754932	0.000816	1.210648
H	-1.804429	0.001389	2.148012
C	-3.755418	-0.000806	-1.210113
H	-1.805271	-0.001383	-2.148238
C	-4.453411	0.000006	0.000404
H	-4.295398	0.001445	2.153180
H	-4.296250	-0.001434	-2.152434
H	-5.540096	0.000007	0.000623

11*

B3LYP SCF energy:	-748.42106975 a.u.
B3LYP enthalpy:	-748.154321 a.u.
B3LYP free energy:	-748.213473 a.u.
M06-2X SCF energy in solution:	-748.33411295 a.u.
M06-2X enthalpy in solution:	-748.067364 a.u.
M06-2X free energy in solution:	-748.126516 a.u.

Cartesian coordinates

ATOM	X	Y	Z
C	-2.649865	-3.032377	0.000036
C	-3.007688	-1.677862	0.000073
C	-1.945663	-0.679537	0.000000
C	-0.573539	-1.129164	-0.000094
C	-0.225577	-2.447967	-0.000125
C	-1.317934	-3.432920	-0.000056
H	-3.432057	-3.787663	0.000082
H	-4.047535	-1.368144	0.000170
H	0.807609	-2.777188	-0.000193
H	-1.062022	-4.487854	-0.000090
C	-1.941192	0.703696	0.000000
C	-2.973666	1.713524	0.000078
C	-2.596789	3.036478	0.000088
C	-1.226479	3.436319	0.000012
C	-0.183967	2.481880	-0.000081
C	-0.538362	1.146962	-0.000088
H	-4.019555	1.422679	0.000132

H	-3.361286	3.809947	0.000151
H	-0.982012	4.494070	0.000024
H	0.856591	2.790037	-0.000139
N	0.251576	0.014940	-0.000184
C	1.683436	-0.002698	-0.000062
C	2.377135	-0.012394	1.214479
C	2.377325	-0.012223	-1.214492
C	3.773082	-0.030963	1.210573
H	1.822666	-0.005218	2.148339
C	3.773274	-0.030788	-1.210373
H	1.822998	-0.004920	-2.148435
C	4.471177	-0.040036	0.000153
H	4.313627	-0.037988	2.152993
H	4.313965	-0.037677	-2.152710
H	5.557739	-0.054233	0.000238

11$^{\bullet+}$

B3LYP SCF energy:	-748.34967442 a.u.
B3LYP enthalpy:	-748.077574 a.u.
B3LYP free energy:	-748.132768 a.u.
M06-2X SCF energy in solution:	-748.25103228 a.u.
M06-2X enthalpy in solution:	-747.978932 a.u.
M06-2X free energy in solution:	-748.034126 a.u.

Cartesian coordinates

ATOM	X	Y	Z
C	-2.572768	-3.041853	0.167502
C	-2.941789	-1.684004	0.091786
C	-1.941208	-0.729533	0.028549
C	-0.581213	-1.137399	0.041325
C	-0.204021	-2.482576	0.148553
C	-1.227927	-3.430167	0.199459
H	-3.349321	-3.799272	0.213673
H	-3.988821	-1.398014	0.089725
H	0.835678	-2.782783	0.201252
H	-0.972890	-4.482227	0.274983
C	-1.941073	0.729802	-0.028422
C	-2.941461	1.684471	-0.091705
C	-2.572157	3.042269	-0.167558
C	-1.227299	3.430280	-0.199622
C	-0.203549	2.482416	-0.148683
C	-0.581058	1.137415	-0.041298
H	-3.988562	1.398736	-0.089596
H	-3.348600	3.799803	-0.213722
H	-0.971976	4.482265	-0.275239
H	0.836210	2.782400	-0.201487
N	0.228711	-0.000132	-0.000014
C	1.647845	-0.000185	0.000027
C	2.339868	0.816916	0.908967
C	2.339901	-0.817243	-0.908927
C	3.731317	0.806642	0.904645

H	1.793470	1.414552	1.630387
C	3.731343	-0.806967	-0.904576
H	1.793504	-1.414811	-1.630408
C	4.429109	-0.000168	0.000052
H	4.271015	1.422957	1.617062
H	4.271079	-1.423207	-1.617031
H	5.515081	-0.000170	0.000051

11-Br$^-$

B3LYP SCF energy:	-3320.39515691 a.u.
B3LYP enthalpy:	-3320.119945 a.u.
B3LYP free energy:	-3320.183519 a.u.
M06-2X SCF energy in solution:	-3322.80850479 a.u.
M06-2X enthalpy in solution:	-3322.533293 a.u.
M06-2X free energy in solution:	-3322.596867 a.u.

Cartesian coordinates

ATOM	X	Y	Z
C	4.612523	0.807131	-1.644982
C	4.202149	-0.400107	-1.084920
C	2.964857	-0.461491	-0.429616
C	2.155427	0.702715	-0.344284
C	2.560526	1.915462	-0.913673
C	3.794962	1.949593	-1.560089
H	5.569876	0.868935	-2.155196

H	4.829530	-1.284947	-1.157364
H	1.936529	2.801217	-0.857778
H	4.129880	2.881216	-2.008691
C	2.238764	-1.523835	0.234254
C	2.516966	-2.874624	0.483625
C	1.586507	-3.639304	1.182753
C	0.384401	-3.064565	1.636025
C	0.082591	-1.724566	1.399739
C	1.017031	-0.961066	0.690675
H	3.448183	-3.316392	0.138017
H	1.788587	-4.688161	1.382088
H	-0.328266	-3.676703	2.182644
H	-0.848533	-1.293562	1.751962
N	0.976141	0.390956	0.337605
C	-0.079669	1.301142	0.644259
C	0.199782	2.481532	1.347698
C	-1.391771	1.013230	0.252070
C	-0.832788	3.372796	1.643713
H	1.216170	2.692260	1.666602
C	-2.420812	1.900765	0.571324
H	-1.648201	0.111186	-0.298896
C	-2.146422	3.083907	1.260622
H	-0.609482	4.287541	2.186786
H	-3.425242	1.629472	0.254054
H	-2.947738	3.778000	1.501356
Br	-4.246126	-0.879973	-1.118971

$11^{\bullet+}$-Br

B3LYP SCF energy:	-3320.21895513 a.u.
B3LYP enthalpy:	-3319.944097 a.u.
B3LYP free energy:	-3320.007120 a.u.
M06-2X SCF energy in solution:	-3322.60331713 a.u.
M06-2X enthalpy in solution:	-3322.328459 a.u.
M06-2X free energy in solution:	-3322.391482 a.u.

Cartesian coordinates

ATOM	X	Y	Z
C	-2.390811	3.074313	-1.182810
C	-2.819495	1.746554	-1.077708
C	-1.877219	0.758374	-0.797262
C	-0.522440	1.118288	-0.608984
C	-0.080418	2.434119	-0.733548
C	-1.038483	3.409270	-1.020500
H	-3.113485	3.855162	-1.401460
H	-3.864833	1.489924	-1.223998
H	0.964296	2.697889	-0.611363
H	-0.725919	4.444753	-1.119332
C	-1.953893	-0.690288	-0.667315
C	-2.999192	-1.608155	-0.757246
C	-2.715856	-2.968075	-0.590665
C	-1.407820	-3.406988	-0.333025
C	-0.349500	-2.502643	-0.231456
C	-0.642366	-1.150144	-0.407201
H	-4.013900	-1.275578	-0.956411

H	-3.520158	-3.694854	-0.660179
H	-1.213119	-4.467612	-0.203587
H	0.657974	-2.840001	-0.013626
N	0.229635	-0.045685	-0.325908
C	1.648077	-0.130604	-0.541810
C	2.128505	-0.882951	-1.622495
C	2.532775	0.574011	0.280976
C	3.500261	-0.929057	-1.871683
H	1.435788	-1.410030	-2.270070
C	3.900887	0.526781	0.015718
H	2.145979	1.111455	1.139789
C	4.388901	-0.223714	-1.057546
H	3.869863	-1.512306	-2.710304
H	4.587462	1.067456	0.660999
H	5.456537	-0.262905	-1.254378
Br	-0.002440	0.177769	2.632361

11-Br-TS1

B3LYP SCF energy:	-3666.59814648 a.u.
B3LYP enthalpy:	-3666.178949 a.u.
B3LYP free energy:	-3666.267797 a.u.
M06-2X SCF energy in solution:	-3668.95077323 a.u.
M06-2X enthalpy in solution:	-3668.531576 a.u.
M06-2X free energy in solution:	-3668.620424 a.u.
Imaginary frequency:	-38.1305 cm-1

Cartesian coordinates

ATOM	X	Y	Z
C	-1.028633	-1.649400	3.817761
C	-1.153083	-2.422070	2.658225
C	-1.442111	-1.781904	1.454042
C	-1.586118	-0.375191	1.427575
C	-1.485241	0.402381	2.580019
C	-1.200117	-0.257774	3.777456
H	-0.805228	-2.134846	4.763442
H	-1.038740	-3.501564	2.697870
H	-1.619295	1.478117	2.555265
H	-1.111696	0.320768	4.692407
C	-1.685324	-2.259987	0.100275
C	-1.692048	-3.526580	-0.482562
C	-1.991148	-3.637960	-1.844402
C	-2.274224	-2.500510	-2.616299
C	-2.262547	-1.223466	-2.052828
C	-1.971699	-1.124950	-0.692176
H	-1.473063	-4.410370	0.109819
H	-2.003111	-4.618436	-2.311656
H	-2.500413	-2.611408	-3.672785
H	-2.463206	-0.343894	-2.654760
N	-1.866137	0.035491	0.103071
C	-2.513045	1.280428	-0.206991
C	-3.838028	1.268425	-0.663462
C	-1.844850	2.492223	-0.002043

C	-4.487980	2.476446	-0.917881
H	-4.358739	0.326796	-0.801539
C	-2.508963	3.692657	-0.250076
H	-0.804115	2.479818	0.302292
C	-3.829077	3.689680	-0.709246
H	-5.514999	2.464308	-1.271488
H	-1.985201	4.632276	-0.098589
H	-4.338777	4.627973	-0.909316
Br	0.948113	0.537689	-0.662195
C	4.587601	1.080995	0.483604
C	4.819476	1.073518	1.955773
H	4.933032	0.057931	2.340974
H	5.715521	1.656472	2.215715
H	3.981440	1.554400	2.484773
C	4.419714	2.378468	-0.240555
H	4.670515	3.226522	0.404740
H	5.040386	2.430761	-1.143864
H	3.377097	2.495744	-0.571707
C	4.443394	-0.188700	-0.209917
O	4.260252	-0.031375	-1.549014
C	3.951842	-1.226891	-2.275718
H	3.009714	-1.655682	-1.922097
H	3.851104	-0.920543	-3.318725
H	4.751080	-1.968229	-2.181487
O	4.489617	-1.295314	0.324341

References

1) Pan, X.; Lamson, M.; Yan, J.; Matyjaszewski, K. *ACS Macro Lett.* **2015,** 4, (2), 192-196.

2) Crivello, J. V. *J. Polym. Sci. A: Polym. Chem.* **2008,** *46*, (11), 3820-3829.

3) Saveant, J. M. *J. Am. Chem. Soc.* **1987,** *109*, (22), 6788-6795.

4) Cardinale, A.; Isse, A. A.; Gennaro, A.; Robert, M.; Savéant, J.-M. *J. Am. Chem. Soc.* **2002,** *124*, (45), 13533-13539.

5) Pause, L.; Robert, M.; Savéant, J.-M. *J. Am. Chem. Soc.* **2000,** *122*, (40), 9829-9835.

6) Pause, L.; Robert, M.; Savéant, J.-M. *J. Am. Chem. Soc.* **2001,** *123*, (21), 4886-4895.

7) Isse, A. A.; Bortolamei, N.; De Paoli, P.; Gennaro, A. *Electrochim. Acta* **2013,** *110*, 655-662.

8) Breu, J.; Stössel, P.; Schrader, S.; Starukhin, A.; Finkenzeller, W. J.; Yersin, H. *Chem. Mater.* **2005,** *17*, (7), 1745-1752.

9) Rehm, D.; Weller, A. *Isr. J. Chem.* **1970,** *8*, (2), 259-271.

10) Riddick, J. A.; Bunger, W. B.; Sakano, T. K. Organic Solvents: Physical Properties and Methods of Purification, 4th Edition 1986, Series Editor: Arnold Weissberger. New York, NY, U.S.A. Wiley-Interscience.

11) Isse, A. A.;Lin, C. Y.; Coote, M. L.; Gennaro, A. *J. Phys. Chem. B* **2011,** *115*, 678-684.

12) Lin, C. Y.; Coote, M. L.; Gennaro, A.;Matyjaszewski, K. *J. Am. Chem. Soc.* **2008,** 130 (38), 12762–12774.

13) Kojima, H.; Bard, A. J. *J. Am. Chem. Soc.* **1975,** *97*, (22), 6317-6324.

14) Donkers, R. L.; Maran, F.; Wayner, D. D. M.; Workentin, M. S. *J. Am. Chem. Soc.* **1999,** *121*, (31), 7239-7248.

15) Saveant, J. M. *J. Am. Chem. Soc.* **1992,** *114*, (26), 10595-10602.

16) D. R. Lide, ed., CRC Handbook of Chemistry and Physics 87th ed.2006, Taylor and Francis, Boca Raton, Florida, US, p. 12-11.

17) Frisch, M. J.; Trucks, G. W.; Schlegel, H. B.; Scuseria, G. E.; Robb, M. A.; Cheeseman, J. R.; Scalmani, G.; Barone, V.; Mennucci, B.; Petersson, G. A.; Nakatsuji, H.; Caricato, M.; Li, X.; Hratchian, H. P.; Izmaylov, A. F.; Bloino, J.; Zheng, G.; Sonnenberg, J. L.; Hada, M.; Ehara, M.; Toyota, K.; Fukuda, R.; Hasegawa, J.; Ishida,

M.; Nakajima, T.; Honda, Y.; Kitao, O.; Nakai, H.; Vreven, T.; Montgomery, J. A., Jr.; Peralta, J. E.; Ogliaro, F.; Bearpark, M.; Heyd, J. J.; Brothers, E.; Kudin, K. N.; Staroverov, V. N.; Kobayashi, R.; Normand, J.; Raghavachari, K.; Rendell, A.; Burant, J. C.; Iyengar, S. S.; Tomasi, J.; Cossi, M.; Rega, N.; Millam, N. J.; Klene, M.; Knox, J. E.; Cross, J. B.; Bakken, V.; Adamo, C.; Jaramillo, J.; Gomperts, R.; Stratmann, R. E.; Yazyev, O.; Austin, A. J.; Cammi, R.; Pomelli, C.; Ochterski, J. W.; Martin, R. L.; Morokuma, K.; Zakrzewski, V. G.; Voth, G. A.; Salvador, P.; Dannenberg, J. J.; Dapprich, S.; Daniels, A. D.; Farkas, Ö.; Foresman, J. B.; Ortiz, J. V.; Cioslowski, J.; Fox, D. J. Gaussian 09, Revision D.01; Gaussian, Inc.: Wallingford, CT, 2009.

18) (a) H.-J. Werner, P. J. Knowles, G. Knizia, F. R. Manby and M. Schütz, *WIREs Comput. Mol. Sci.* **2012**, *2*, 242-253. (b) MOLPRO, version 2012.1, a package of ab initio programs, H.-J. Werner, P. J. Knowles, G. Knizia, F. R. Manby, M. Schütz, P. Celani, T. Korona, R. Lindh, A. Mitrushenkov, G. Rauhut, K. R. Shamasundar, T. B. Adler, R. D. Amos, A. Bernhardsson, A. Berning, D. L. Cooper, M. J. O. Deegan, A. J. Dobbyn, F. Eckert, E. Goll, C. Hampel, A. Hesselmann, G. Hetzer, T. Hrenar, G. Jansen, C. Köppl, Y. Liu, A. W. Lloyd, R. A. Mata, A. J. May, S. J. McNicholas, W. Meyer, M. E. Mura, A. Nicklass, D. P. O'Neill, P. Palmieri, D. Peng, K. Pflüger, R. Pitzer, M. Reiher, T. Shiozaki, H. Stoll, A. J. Stone, R. Tarroni, T. Thorsteinsson, and M. Wang, , see http://www.molpro.net.

19) Böes, E. S.; Livotto, P. R.; Stassen, H. *Chem. Phys.***2006**, *331*, 142-158.

20) Marenich, A. V.; Cramer, C. J.; Truhlar, D. G. *J. Phys. Chem. B* **2009**, *113*, 6378–6396

21) Kowert, B. A.; Marcoux, L.; Bard, A. J. *J. Am. Chem. Soc.* **1972,** *94*, (16), 5538-5550.

22) Youcheng, W. L. G. X. W. J. G. Q. L. Z. L. *SCIENCE CHINA Chemistry* **1999,** *42*, (2), 138-144.

23) (a) R.C. Tolman, Statistical Mechanics, Chemical Catalog Co, New York, 1927, p. 247. (b) J.R. Partington, An Advanced Treatise on Physical Chemistry, vol. 1, Longmans, London, 1967, p. 292. (c) J.W. Moore, R.N. Pearson, Kinetics and Mechanism, vol. 131, Wiley, New York, 1981, p. 130.

24) Savéant, J.-M. *J. Electroanal. Chem.* **2000,** *485*, (1), 86-88.

25) J.W. Moore, R.N. Pearson, Kinetics and Mechanism, vol. 131, Wiley, New York, 1981, p. 130.
26) Shine, H. J.; Silber, J. J.; Bussey, R. J.; Okuyama, T. *J. Org. Chem.* **1972,** *37*, (17), 2691-2697.
27) Laidler, K. J. *Chemical Kinetics*, 3rd ed., Harper & Row, Publishers Inc., 1987, p. 216.